Mechanics of Materials 157 (2021) 103796

Contents lists available at ScienceDirect

Mechanics of Materials

journal homepage: www.elsevier.com/locate/mechmat

# Broadband dynamic elastic moduli of honeycomb lattice materials: A generalized analytical approach

S. Adhikari [a], T. Mukhopadhyay [b,*], X. Liu [c]

[a] Future Manufacturing Research Centre, College of Engineering, Swansea University, Swansea, UK
[b] Department of Aerospace Engineering, Indian Institute of Technology Kanpur, Kanpur, India
[c] Key Laboratory of Traffic Safety on Track, Ministry of Education, School of Traffic & Transportation Engineering, Central South University, Changsha, China

ARTICLE INFO

*Keywords:*
Frequency-dependent dynamic elastic moduli
Dynamic stiffness for Timoshenko beams
Elastic moduli of lattice metamaterials
Axial and shear deformation effects in lattices
Non-prismatic beam networks

ABSTRACT

A generic analytical framework is proposed to obtain the dynamic elastic moduli of lattice materials under steady-state vibration conditions. The dynamic deformation behaviour of the individual beam elements of a lattice is distinct from the behaviour under a static condition. This leads to a completely different global deformation pattern of the lattice material and subsequently opens up a tremendous opportunity to modulate amplitude and phase of the elastic properties of lattices as a function of the ambient vibration. The dynamic stiffness approach proposed in this article precisely captures the sub-wavelength scale dynamics of the periodic network of beams in a lattice material using a single beam-like member. Here the dynamic stiffness matrix of a damped beam element based on the Timoshenko beam theory along with axial stretching is coupled with the unit cell-based approach to derive the most general closed-form analytical formulae for the elastic moduli of lattice materials across the whole frequency range. It is systematically shown how the general expressions of dynamic elastic moduli can be reduced to different special cases by neglecting axial and shear deformations under dynamic as well as classical static conditions. The significance of developing the dynamic stiffness approach compared to conventional dynamic finite element approach is highlighted by presenting detailed analytical derivations and representative numerical results. Further, it is shown how the analytical framework can be readily extended to lattices with non-prismatic beam elements with any spatial variation in geometry and intrinsic material properties. In general, research activities in the field of lattice metamaterials dealing with elastic properties revolve around intuitively designing the microstructural geometry of the lattice structure. Here we propose to couple the physics of deformation as a function of vibrating frequency along with the conventional approach of designing microstructural geometry to expand the effective design space significantly. The stretching-enriched physics of deformation in the lattice materials in addition to the bending and shear deformations under dynamic conditions lead to complex-valued elastic moduli due to the presence of damping in the constituent material. The amplitude, as well as the phase of effective elastic properties of lattice materials, can be quantified using the proposed approach. The dependence of Poisson's ratio on the intrinsic material physics in case of a geometrically regular lattice is found to be in contrary to the common notion that Poisson's ratios of perfectly periodic lattices are only the function of microstructural geometry. The generic analytical approach for analysing the elastic moduli is applicable to any form of two- or three-dimensional lattices, and any profile of the constituent beam-like elements (different cross-sections as well as spatially varying geometry and intrinsic material properties) through a wide range of frequency band. The closed-form expressions of elastic moduli derived in this article can be viewed as the broadband dynamic generalisation of the well-established classical expressions of elastic moduli under static loading, essentially adding a new exploitable dimension in the metamaterials research in terms of dynamics of the intrinsic material.

* Corresponding author.
*E-mail address:* tanmoy@iitk.ac.in (T. Mukhopadhyay).

https://doi.org/10.1016/j.mechmat.2021.103796
Received 18 May 2020; Received in revised form 17 November 2020; Accepted 5 February 2021
Available online 18 February 2021

## 1. Introduction

Lattice-based materials are a class of mechanical metamaterials which are typically characterised by the periodicity of a unit cell. An interesting aspect of such metamaterials is that the overall property is largely dependent on the geometric features of the periodic unit cells besides the intrinsic property of the constituent material. Intense research in recent years show exciting and unprecedented developments such as ultralight metamaterials (Zheng et al., 2014) approaching theoretical strength limit (Berger et al., 2017), pentamode materials (Kadic et al., 2012) with cloaking mode (Buckmann et al., 2014), negative refraction elastic waves (Zhu et al., 2014), far-field actuation dependent local shape and stiffness modulation (Mukhopadhyay et al., 2020a; Wang et al., 2020), elastic cloaking (Milton et al., 2006; Stenger et al., 2012), hyperbolic elastic metamaterials (García-Chocano et al., 2014), negative Poisson's ratio (auxetic) materials (Lakes, 1987; Mukhopadhyay and Adhikari, 2017a), materials with negative effective elastic modulus (Fang et al., 2006), negative mass density (Yang et al., 2008), multi-physical and multi-material property modulation (Mukhopadhyay et al., 2019a, 2020b; Singh et al., 2021) and nano-scale multi-functional properties (Chandra et al., 2020; Mukhopadhyay et al., 2017a, 2018, 2020c; Roy et al., 2021). Such advanced materials are often used in vibrating systems such as aerospace structures, wind turbine and a plenty of electro-mechanical devices. In a vibrating condition, deformation behaviour of the individual beam elements of a lattice material becomes significantly different from the behaviour under a static condition. This leads to a completely different global deformation behaviour of the lattice material and subsequently the effective elastic properties such as Young's moduli, shear modulus and Poisson's ratios become dependent on the vibration parameters. Focus of this article is to investigate the effective elastic properties of lattice materials as a function of vibrating frequencies covering a broad brand.

A unit cell (or representative volume element) based approach to obtain effective properties (also know as homogenisation methods) of periodic elastic materials can be traced back to the classical work by Hashin and Shtrikman (1963). Exploiting periodic boundary conditions and mechanics of a unit cell, equivalent mechanical properties for cellular materials have been investigated in (El-Sayed et al., 1979; Gibson and Ashby, 1999; Malek and Gibson, 2015; Meza et al., 2017; Mukhopadhyay et al., 2017b; Wehmeyer et al., 2019; Zok et al., 2016; Zschernack et al., 2016)), (), (. Homogenisation of metamaterials with sub-wavelength dynamics needs to differ from the classical homogenisation approaches due to the fact that there are local resonators embedded in metamaterials. This has led to the development of dynamic homogenisation approaches (Nemat-Nasser et al., 2011; Norris et al., 2012; Willis, 2009; Craster et al., 1098). The dynamic homogenisation can be viewed as a higher-order method (Srivastava, 2015) compared to the classical static homogenisation approaches. The unit cell based homogenisation approaches are strictly not applicable when the lattices are not perfectly periodic, as will be the case when random inhomogeneities are present in the metamaterial. To address this issue, the idea of 'representative unit cell element (RUCE) was introduced (Mukhopadhyay and Adhikari, 2017b; Mukhopadhyay and Adhikari, 2016a) in the context of static homogenisation of cellular metamaterials. This approach is a step-change in the field as it provides the analytical basis for considering inhomogeneities in cellular metamaterials and develops closed-form physics-based expressions for equivalent (static) elastic properties. The effective out-of-plane elastic properties of randomly disordered lattices are shown in (Mukhopadhyay and Adhikari, 2016b). Homogenisation of continuum systems with random circular inclusions have been discussed recently (Pivovarov and Steinmann, 2016a,b) for static problems.

Vibration and wave propagation in periodic structures (Brillouin, 1953) plays a crucial role in the analysis and design of metamaterials. Extensive works have been undertaken since the mid 60's on dynamics of periodic structures (Mead, 1996). The main motivation was to efficiently analyse large aerospace structures made of periodic units such as periodically stiffened shell in an aircraft fuselage. One of the most popular computational methods for analysing wave propagation in metamaterials rely on the Floquet-Bloch theorem (Hussein et al., 2014), which is essentially based on periodic boundary condition for a unit cell. Overall wave propagation behaviour depends on the dynamic characteristics of a unit cell and can be understood in terms of the band-gaps (Deymier, 2013), (Brillouin, 1953). Consequently, efficient analytical methods (Bigoni et al., 2013) and numerical methods for the computation of bandgaps of metamaterials have taken centre stage in most current research (Hussein, 2009a; Palermo and Marzani, 2016; Sugino et al., 2016). Classical wave propagation approaches were developed for undamped metamaterials. Few authors have considered damped metamaterials (Hussein, 2009b) where internal damping within a unit cell is considered explicitly (Hussein and Frazier, 2013; Yu et al., 2017).

Dynamic elastic moduli of metamaterials differ from the effective elastic moduli under a static condition (Mukhopadhyay et al., 2019b). Such dynamic elastic moduli are a function of the forcing frequency of vibration. The difference is due to the fact that deformation behaviour of the constituting members (such as the beam indicated in Fig. 1) is different in static and dynamic environments. This essentially leads to a significant deviation (/enhancement) in elastic moduli of lattice materials, which is actually a network of such constituent members. The enhanced elastic moduli has been proposed to be exploited in the optimum design of various structural systems (such as aircraft wings and turbine blades), which are subjected to vibration during the operational condition (Mukhopadhyay et al., 2019b). It can be shown that the elastic moduli could become negative at certain frequencies depending on the microstructural configuration. In a recent paper, the sub-wavelength scale dynamics in the deformation of a constituent beam element has been captured based on dynamic stiffness approach considering only bending deformation. This has led to the derivation of closed-form analytical limits of negative elastic moduli (Adhikari et al., 2020; Mukhopadhyay et al., 2019c). In this context, it is important to note that three contributing mechanisms in the effective deformation of lattice materials are bending, shear and axial, among which bending deformation is normally predominant in the static elastic moduli for thin cell-walled hexagonal lattices. Such lattices can effectively be analysed using the Euler-Bernoulli beam theorem. However, even in case of thin cell-walled lattices, the shear and axial deformation can assume significant role in case of higher frequencies. Thus the previous analytical framework (Mukhopadhyay et al., 2019b) is essentially restricted to the low frequency range and thin cell walls.

In this paper we aim to develop a generic analytical framework applicable to a broad band of frequency based on Timoshenko beam formulation (Bhat and Ganguli, 2019; Dawe, 1984) coupled with the dynamic stiffness approach, wherein all the three deformation mechanisms (bending, axial and shear) can be accounted. Thus the proposed formulation will be applicable to static as well as higher frequencies of vibration without any restriction of cell wall thickness. First, the dynamic stiffness of a single beam element is developed based on Timoshenko beam theory and thereafter, the dynamic stiffness matrix of a single beam element will be utilized to obtain the effective elastic properties of the entire periodic lattice on the basis of unit cell approach (refer to Fig. 1(a–c)). Most of the research activities in the field of lattice metamaterials dealing with elastic properties revolve around intuitively designing the microstructural geometry of the lattice structure. Here we essentially propose to couple the physics of deformation as a function of vibrating broad band frequency along with the conventional approach of designing microstructural geometry to expand the effective design space significantly. In the following sections, first a detailed derivation of the effective frequency-dependent elastic properties of lattice materials (including the derivation of static and dynamic stiffness matrices for a single beam element and the effective elastic properties of the entire lattice there after) is presented along with insightful numerical results, followed by discussions on several special cases and generality of

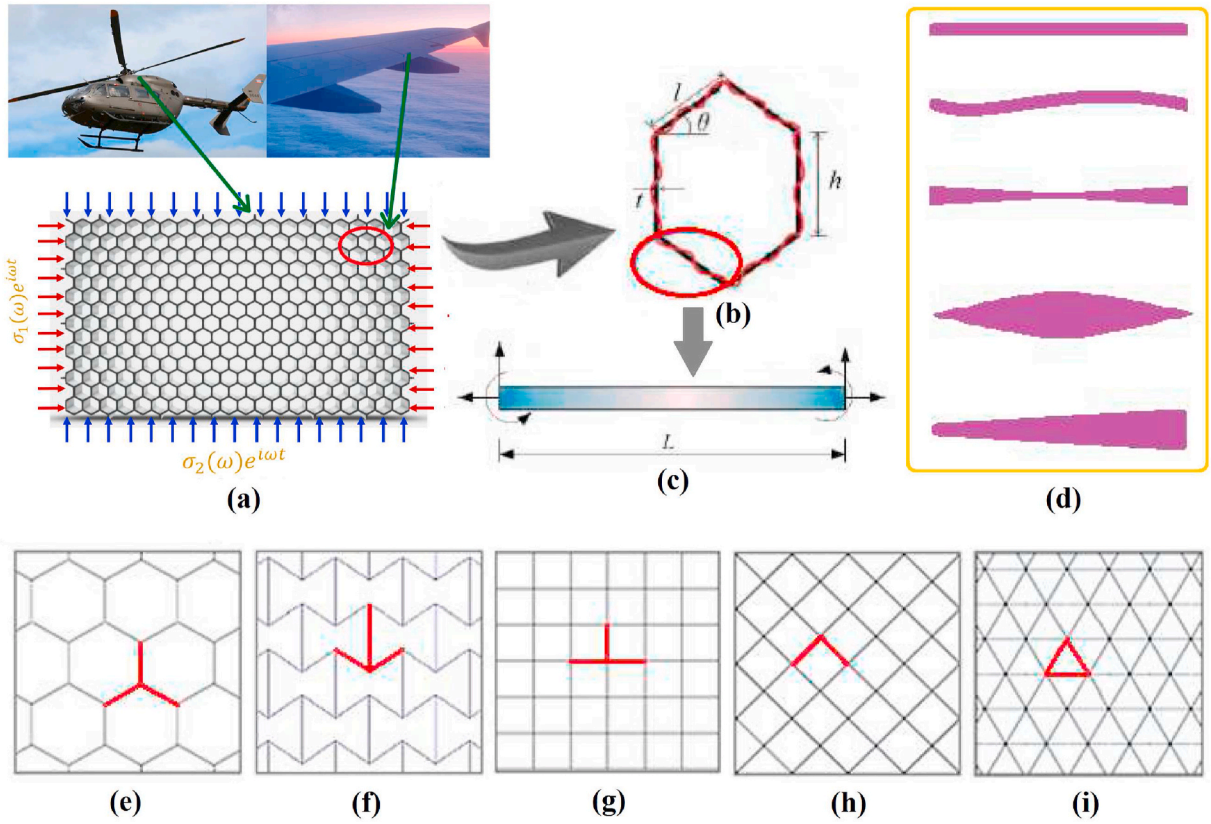


**Fig. 1.** Generic lattice metamaterials under vibrating condition. (a) Typical representation of a generic lattice metamaterial under dynamic loading (such as the honeycomb core as a part of sandwich structures used in aircraft components). Here we show a multi-scale framework starting from the macro-structure level of an aircraft to the microstructure level of the honeycomb. (b) Hexagonal unit cell under vibration, where the deformation mechanism of each constituent beam elements are different from their static counterpart (c) A Timoshenko beam element with two nodes and six degrees of freedom consisting of the axial deformation, transverse deformation and rotation at the two nodes. Here the displacement field in between the two nodes is expressed using complex frequency-dependent shape functions. (d) Typical representation of different beam shapes which could potentially be used as constituent beams in proposed analytical framework (e–i) Different types of lattices where the proposed analytical approach could be readily applicable (the respective unit cells are highlighted).

the proposed framework, and concluding remarks.

## 2. Overview of the unit cell approach for equivalent elastic moduli

### 2.1. Equivalent in-plane elastic moduli

The effective elastic properties of a lattice material is important for global stress-strain analysis. When in-plane elasticity of orthotropic 2D materials are considered, the constitutive relationship can be expressed as (Rivello, 1969)

$$\begin{Bmatrix} \varepsilon_{11} \\ \varepsilon_{22} \\ 2\varepsilon_{12} \end{Bmatrix} = \begin{bmatrix} 1/E_1 & -\nu_{21}/E_2 & 0 \\ -\nu_{12}/E_1 & 1/E_2 & 0 \\ 0 & 0 & 1/G_{12} \end{bmatrix} \begin{Bmatrix} \sigma_{11} \\ \sigma_{22} \\ \sigma_{12} \end{Bmatrix} \tag{1}$$

Here $\varepsilon_{(\cdot)}$ and $\sigma_{(\cdot)}$ represent strain and stress within the 2D material. In the above equation $E_1$ is the longitudinal Young's modulus, $E_2$ is the transverse Young's modulus, $G_{12}$ is the shear modulus, $\nu_{12}$ and $\nu_{21}$ are the Poisson's ratios. These five quantities explicitly define stress-strain relationship. This can be illustrated by inverting the coefficient matrix in Eq. (1) as

$$\begin{Bmatrix} \sigma_{11} \\ \sigma_{22} \\ \sigma_{12} \end{Bmatrix} = \begin{bmatrix} E_1/(1-\nu_{12}\nu_{21}) & \nu_{21}E_1/(1-\nu_{12}\nu_{21}) & 0 \\ \nu_{12}E_2/(1-\nu_{12}\nu_{21}) & E_2/(1-\nu_{12}\nu_{21}) & 0 \\ 0 & 0 & G_{12} \end{bmatrix} \begin{Bmatrix} \varepsilon_{11} \\ \varepsilon_{22} \\ 2\varepsilon_{12} \end{Bmatrix} \tag{2}$$

We consider the case when external stress or strain applied to the material is dynamic in nature. Without any loss of generality, the steady-state condition is assumed along with the fact that the applied excitation is harmonic in nature. Considering the linear material behaviour, we can deduce that both stress and strain will be functions of a same frequency value. From Eq. (2) we can therefore obtain

$$\begin{aligned} \sigma_{11}(\omega) &= \frac{E_1(\omega)}{(1-\nu_{12}(\omega)\nu_{21}(\omega))}(\varepsilon_{11}(\omega)+\nu_{21}(\omega)\varepsilon_{22}(\omega)) \\ \sigma_{22}(\omega) &= \frac{E_2(\omega)}{(1-\nu_{12}(\omega)\nu_{21}(\omega))}(\nu_{12}(\omega)\varepsilon_{11(\omega)}+\varepsilon_{22}(\omega)) \\ \sigma_{12}(\omega) &= G_{12}(\omega)[2\varepsilon_{12}(\omega)] \end{aligned} \tag{3}$$

In this expression, all the five elasticity constants (three elastic moduli and two Poisson's ratios) are frequency dependent. The aim of this paper is to derive analytical expressions of these quantities. The frequency depended elasticity constants have some advantages over the classical 'static' elastic constants for 2D lattices:

- *Physical insights:* The frequency depended elasticity constants give a more comprehensive characterization of these crucial material constants as the excitation frequency changes. The 'static' elastic constants appear as a special case when the frequency is 'zero'. The adaptive nature of the materials constants in the frequency domain gives rise to exciting new physical phenomenon such as negative elastic moduli at certain frequency ranges (Adhikari et al., 2020; Mukhopadhyay et al., 2019c), negative mass density (Chen et al., 2017) and anisotropic mass density (Zhu et al., 2016).
- *Quantification of damping:* Due to the presence of damping in the microstructure, the material constants become complex-valued

functions in the frequency domain. This gives a direct route to quantify damping of the overall material. This is in general not possible if classical elastic constants are used.

- *Computational advantage:* Dynamic analysis of complex systems with embedded cellular materials is governed by boundary value problems. In general, some numerical methods such as the finite element method are necessary to solve such problems. The use of frequency dependent elasticity constants will allow coarser discretization leading to an efficient computational approach. This is possible because frequency dependent elasticity constants take account of inertia properties and localised vibration modes accurately.

  Frequency-dependent elasticity constants, therefore, quantify equivalent homogeneous properties of 2D lattices when subjected to external harmonic excitation. Although the equivalent homogeneous properties are considered here, another area where the proposed formation will be relevant is the in-plane wave propagation (Karlicic et al., 2021; Liu et al., 2011). Here frequency dependent elasticity constants can be incorporated for enhanced computational efficiency and accuracy.

### 2.2. The unit cell model

The effective elastic property of a lattice structure can be obtained by exploiting the periodicity of a suitably selected unit cell. The choice of the unit cell is not unique. If a two-dimensional lattice is perfectly periodic in both the directions and there are a sufficient number of unit cells, the equivalent elastic properties are independent of the choice of the unit cell as long as it physically represents the entire lattice structure. Therefore, it is customary to choose a unit cell which simplifies the analysis. In Fig. 2 we show a representative example of a hexagonal lattice and its corresponding unit cell. Each of the cell walls bend and stretch when subjected to in-plane stress. When the applied stress is uniform along with the out of plane, each elements of the unit cell in Fig. 2(b) can be modelled as a beam. Here we briefly discuss the statics and dynamics of beams using different standard approaches. Two different types of beam theories, namely, Euler-Bernoulli beam theory and Timoshenko beam theory will be covered. For each of the beam theories, three different ways of modelling the deformation will be investigated - (a) static deformation, (b) dynamics using the conventional finite element approach, and (c) the dynamic stiffness approach. These three approaches are ordered in the degree of higher fidelity. The static analysis can be considered as a special case of a dynamic analysis when the frequency is zero. For the dynamic analysis in general we consider that the system is damped. This, in turn, will result in complex system matrices.

### 2.3. The beam elements for static analysis

In this subsection we have briefly presented the beam stiffness matrices under static condition for the sake of completeness. It may noted that this particular subsection is not novel; however, it is kept in this paper concisely to maintain the flow of understanding and chronological development of the research topic.

#### 2.3.1. Euler-Bernoulli beam element

The equation governing the transverse deflection of a beam modelled using the Euler-Bernoulli beam theory (Dawe, 1984) is given by

$$EI\frac{\partial^4 w}{\partial x^4}=f_b \tag{4}$$

Here $w \equiv w(x)$ and $f_b \equiv f_b(x)$ are the transverse displacement and applied transverse forcing on the beam. The quantity $EI$ is the bending stiffness of the beam, $I$ is the inertia moment of the beam cross section and $E$ is the Young's modulus of the beam material (i.e. intrinsic material property). If the axial deformation is considered, the equation governing is expressed as

$$EA\frac{\partial^2 u}{\partial x^2}=f_a \tag{5}$$

where $u \equiv u(x)$ and $f_a \equiv f_a(x)$ are the axial displacement and applied axial forcing on the beam. Here $EA$ is the axial stiffness of the beam and $A$ is the area of the beam cross-section. It is well known that the force-displacement relationship of a beam element governed by the above two differential equation can be *exactly* represented using the finite element formulation with cubic shape function for the bending and linear shape function for the axial deformation. A beam element of length $L$ is shown in Fig. 3 with two nodes and three degrees of freedom per node. The degrees of freedom in each node corresponds to the axial, transverse and rotational deformation. The stiffness matrix (Dawe, 1984; Petyt, 1990) of the beam element in Fig. 3 can be expressed by

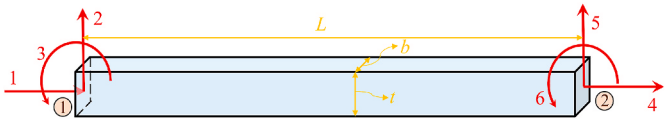


**Fig. 3.** A beam element with six degrees of freedom and two nodes. The degrees of freedom in each node corresponds to the axial, transverse and rotational deformation.

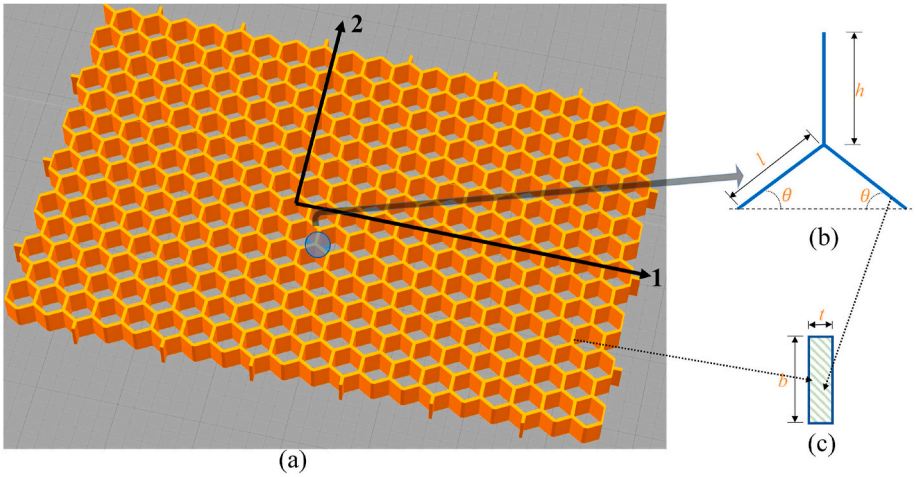


**Fig. 2.** (a) Typical representation of a hexagonal lattice (b) The unit cell considered in this paper. Dimensions of the three-beam element are shown in the figure (c) The out of plane cross-section of each beam element.

$$\mathbf{K}_s = \begin{bmatrix} \frac{EA}{L} & 0 & 0 & -\frac{EA}{L} & 0 & 0 \\ 0 & \frac{12EI}{L^3} & \frac{6EI}{L^2} & 0 & -\frac{12EI}{L^3} & \frac{6EI}{L^2} \\ 0 & \frac{6EI}{L^2} & \frac{4EI}{L} & 0 & -\frac{6EI}{L^2} & \frac{2EI}{L} \\ -\frac{EA}{L} & 0 & 0 & \frac{EA}{L} & 0 & 0 \\ 0 & -\frac{12EI}{L^3} & -\frac{6EI}{L^2} & 0 & \frac{12EI}{L^3} & -\frac{6EI}{L^2} \\ 0 & \frac{6EI}{L^2} & \frac{2EI}{L} & 0 & -\frac{6EI}{L^2} & \frac{4EI}{L} \end{bmatrix} \tag{6}$$

The subscript $s$ in the above equation denotes the fact that the stiffness matrix is obtained using the shape functions satisfying the governing equations of static deformation. The displacements corresponding to degrees of freedom 1 and 4 correspond to the axial deformation governed by Eq. (5), while the displacements corresponding to degrees of freedom 2, 3, 5 and 6 correspond to the bending deformation governed by Eq. (4).

### 2.3.2. Timoshenko beam element

The equations governing the transverse deflection (Dawe, 1984) of a beam modelled using the Timoshenko beam theory are given by

$$kAG\frac{\partial}{\partial x}\left(\frac{\partial w}{\partial x}-\theta\right)=0 \quad \text{and} \quad EI\frac{\partial^2\theta}{\partial x^2}+kAG\left(\frac{\partial w}{\partial x}-\theta\right)=f_b \tag{7}$$

Here $\theta \equiv \theta(x)$ is the rotation of the beam, $kAG$ is the shear stiffness with $G$ as the shear modulus and $k$ is the shear area coefficient. For solid rectangular sections $k = 5/6$ and for solid circular sections $k = 9/10$. Following the conventional finite element method, it can be shown that the stiffness matrix (Dawe, 1984; Petyt, 1990) of the Timoshenko beam element can be expressed as

$$\mathbf{K}_s = \begin{bmatrix} \frac{EA}{L} & 0 & 0 & -\frac{EA}{L} & 0 & 0 \\ 0 & 12\frac{EI}{(1+\Phi)L^3} & 6\frac{EI}{(1+\Phi)L^2} & 0 & -12\frac{EI}{(1+\Phi)L^3} & 6\frac{EI}{(1+\Phi)L^2} \\ & 6\frac{EI}{(1+\Phi)L^2} & \frac{(4+\Phi)EI}{(1+\Phi)L} & 0 & -6\frac{EI}{(1+\Phi)L^2} & \frac{(2-\Phi)EI}{(1+\Phi)L} \\ -\frac{EA}{L} & 0 & 0 & \frac{EA}{L} & 0 & 0 \\ 0 & 12\frac{EI}{(1+\Phi)L^3} & -6\frac{\mathrm{EI}}{(1+\Phi)L^2} & 0 & 12\frac{EI}{(1+\Phi)L^3} & -6\frac{EI}{(1+\Phi)L^2} \\ 0 & 6\frac{EI}{(1+\Phi)L^2} & \frac{(2-\Phi)EI}{(1+\Phi)L} & 0 & -6\frac{EI}{(1+\Phi)L^2} & \frac{(4+\Phi)EI}{(1+\Phi)L} \end{bmatrix} \tag{8}$$

The term $\Phi$ gives the relative importance of the shear deformations to the bending deformations. For a rectangular cross-section

$$\Phi = \frac{12EI}{kAGL^2} = \frac{2(1+\nu)}{k}\left(\frac{t}{L}\right)^2 \tag{9}$$

Here is $\nu$ is the Poisson's ratio of the beam material and we have used the relationships

$$G = E/2(1+\nu) \tag{10}$$

$$I = \frac{1}{12}bt^3 \tag{11}$$

$$A = bt \tag{12}$$

Shear deformation effects are significant for beams which have a length-to-depth ratio less than 5. To neglect the shear deformation, we set $\Phi = 0$. In this case, the stiffness matrix given here reduces to the classical stiffness matrix of the Euler-Bernoulli beam given in the preceding subsection. Therefore, Timoshenko beam model can be viewed as a generalisation of the Euler-Bernoulli beam theory in the static regime. In the following subsections, we will show as to how the static formulation of beams can be further generalized for dynamic conditions.

## 2.4. The beam elements for dynamic analysis

For dynamic analysis using the finite element method, the mass matrix of the beam is necessary. The mass matrix $\mathbf{M}_s$ can be obtained using the same shape functions used to derive the element stiffness matrices given in the previous section using the standard finite element procedure. Using the mass, damping and stiffness matrices, the element dynamic matrix can be obtained as

$$\mathbf{D}_s(\omega) = -\omega^2\mathbf{M}_s + \mathrm{i}\omega\mathbf{C}_s + \mathbf{K}_s \tag{13}$$

where ω is the frequency of excitation, $\mathbf{C}_s$ is the damping matrix and $\mathrm{i} = \sqrt{-1}$ is the unit imaginary number. The dynamic equilibrium equation corresponding to the above element dynamic matrix can be expressed as

$$\mathbf{D}_s(\omega)\mathbf{U}_e(\omega) = \mathbf{f}_e(\omega) \tag{14}$$

Here $\mathbf{U}_e(\omega)$ and $\mathbf{f}_e(\omega)$ are respectively the nodal displacement and applied forcing vector on the element. In general both vectors are complex valued.

The stiffness matrix appearing in Eq. (13) is given in the previous section for two types of beam elements. The mass matrix (Dawe, 1984; Petyt, 1990) for the Euler-Bernoulli beam element is given by

$$\mathbf{M}_s = \frac{\rho AL}{420}\begin{bmatrix} 140 & 0 & 0 & 70 & 0 & 0 \\ 0 & 156 & 22L & 0 & 54 & -13L \\ 0 & 22L & 4L^2 & 0 & 13L & -3L^2 \\ 70 & 0 & 0 & 140 & 0 & 0 \\ 0 & 54 & 13L & 0 & 156 & -22L \\ 0 & -13L & -3L^2 & 0 & -22L & 4L^2 \end{bmatrix} \tag{15}$$

For the Timoshenko beam element, the mass matrix (Dawe, 1984), (Petyt, 1990) can be expressed as

$$\mathbf{M}_s = \frac{\rho AL}{840}\begin{bmatrix} 280 & 0 & 0 & 140 & 0 & 0 \\ & 312+588\Phi+280\Phi^2 & (44+77\Phi+35\Phi^2)L & 0 & 108+252\Phi+175\Phi^2 & -(26+63\Phi+35\Phi^2)L \\ & & (8+14\Phi+7\Phi^2)L^2 & 0 & (26+63\Phi+35\Phi^2)L & -(6+14\Phi+7\Phi^2)L^2 \\ & & & 280 & 0 & 0 \\ & \text{Sym} & & & 312+588\Phi+280\Phi^2 & -(44+77\Phi+35\Phi^2)L \\ & & & & & (8+14\Phi+7\Phi^2)L^2 \end{bmatrix} \tag{16}$$

To neglect the shear deformation, we set $\Phi = 0$.in which case the mass matrix given in Eq. (16) reduces to the mass stiffness matrix of the Euler-Bernoulli beam given in Eq. (15). The damping matrix can be obtained using the finite element method similar to the mass and stiffness matrices. However, often damping matrix is expressed in terms of he mass and stiffness matrices. If Rayleigh damping model is used (see for example (Adhikari, 2013))), then the damping matrix can be expressed as

$$\mathbf{C}_s = c_k\mathbf{K}_s + c_m\mathbf{M}_s \tag{17}$$

Here $c_m$ and $c_k$ are mass and stiffness proportional damping coefficients. Using this damping matrix, the element dynamic matrix from (13) can be rewritten as

$$\mathbf{D}_s(\omega) = (1 + \mathrm{i}\omega c_k)\mathbf{K}_s + \left(-\omega^2 + \mathrm{i}\omega c_m\right)\mathbf{M}_s \tag{18}$$

All the elements of this $6 \times 6$ matrix can be obtained for both Euler-Bernoulli and Timoshenko beam elements using the respective expressions of the mass and stiffness matrices. This matrix will be referred as dynamic finite element matrix differentiating with the static stiffness matrix discussed in the previous section. Indeed, for the special case of static defamation, setting the frequency $\omega = 0$, this dynamic finite element matrix reduces to the conventional static stiffness matrix, as expected.

The dynamic element matrix given in Eq. (18) is derived using the shape function for static deformation of the beam. Therefore, it cannot be used for higher frequency unless the beam is discretised into a fine mesh. Although the procedure is rather straightforward, it will not give closed-form expressions we are seeking in this paper. Moreover, a fine discretization makes the analysis computationally quite intensive. In the next section, dynamic stiffness matrix method is discussed which uses the exact shape function satisfying the governing differential equations.

### 2.5. Dynamic stiffness analysis of beams

The dynamic stiffness method was first proposed by Kolouŝek in 1940's (Kolouŝek, 1941) with many synonyms such as spectral element method (Lee, 2009), spectral finite element method (Gopalakrishnan et al., 2008) etc. One of the most important properties of the dynamic stiffness method (Leung, 1993) is that its shape functions are essentially the exact general solutions derived from the differential equation governing structural vibration in the frequency domain. There is no approximation involved based on the governing differential equation and therefore, only a single dynamic stiffness element can be used to describe the deformation of an element within the whole frequency range without resorting to discretization. Another important property is that the dynamic stiffness matrix is of analytical essence whose elements are transcendental functions of frequency instead of separated stiffness and mass matrices as in the finite element method. The mass distribution of the elements in the dynamic stiffness method is treated in an exact manner for deriving the element dynamic stiffness matrix. The dynamic stiffness matrix of one-dimensional structural elements, taking into account the effects of flexure, torsion, axial and shear deformation, and damping, is exactly determinable, which, in turn, enables the exact vibration analysis by an inversion of the global dynamic stiffness matrix. The method does not employ eigenfunction expansions and, consequently, a major step of the traditional finite element analysis, namely, the determination of natural frequencies and mode shapes, is eliminated which avoids the errors due to series truncation. The method is essentially a frequency-domain approach suitable for steady-state harmonic or stationary random excitation problems.

In what follows, the analytical expressions of the dynamic stiffness formulations are provided for both the axial vibration and bending vibration (both Euler-Bernoulli and Timoshenko theories) of a beam element as shown in Fig. 3.

#### 2.5.1. Axial vibration

The equation governing axial motion (Leung, 1993; Paz, 1980; Petyt, 1990) of a beam is

$$EA\left(1 + \zeta_k\frac{\partial}{\partial t}\right)\frac{\partial^2 u}{\partial x^2} - \rho A\frac{\partial^2 u}{\partial t^2} - c_a\frac{\partial u}{\partial t} = 0 \tag{19}$$

and the axial force boundary condition is

$$N(x) = EA(1 + \zeta_k\partial/\partial t)\partial u/\partial x \tag{20}$$

in which, $EA$ is the stiffness for axial deformation, $\rho A$ is mass per unit length, $\zeta_k$ is the stiffness proportional damping factor, $c_a$ is the velocity-dependent viscous damping coefficient. By introducing the non-dimensional length $\xi = x/L$ and harmonic vibration assumption $u(x,t) = U(x)e^{i\omega t}$, one has the characteristic equation

$$\frac{\mathrm{d}^2 U}{\mathrm{d}\xi^2} + k_a^2 U = 0 \tag{21}$$

where

$$k_a^2 = \frac{(\rho A\omega^2 - i\omega c_a)L^2}{EA(1 + i\omega\zeta_k)} = \frac{\rho\omega^2 L^2(1 - i\zeta_{ma}/\omega)}{E(1 + i\omega\zeta_k)} \tag{22}$$

and $\zeta_{ma} = c_a/(\rho A)$ is the mass proportional damping factor for axial vibration. The exact shape function can be derived

$$U(\xi) = c_1\cos(k_a\xi) + c_2\sin(k_a\xi) \tag{23}$$

Therefore, the displacement boundary conditions for a beam element can be written in the matrix form as

$$\begin{bmatrix} U_1 \\ U_2 \end{bmatrix} = \begin{bmatrix} U(\xi = 0) \\ U(\xi = 1) \end{bmatrix} = \begin{bmatrix} 1 & 0 \\ \cos(k_a) & \sin(k_a) \end{bmatrix}\begin{bmatrix} c_1 \\ c_2 \end{bmatrix} \tag{24}$$

whereas the force boundary conditions can be given as

$$\begin{bmatrix} N_1 \\ N_2 \end{bmatrix} = \begin{bmatrix} -N(\xi = 0) \\ N(\xi = 1) \end{bmatrix} = \frac{EA(1 + i\omega\zeta_k)k_a}{L}\begin{bmatrix} 0 & -1 \\ -\sin(k_a) & \cos(k_a) \end{bmatrix}\begin{bmatrix} c_1 \\ c_2 \end{bmatrix} \tag{25}$$

Eliminating the unknowns $c_1, c_2$ leads to the dynamic stiffness formulation for the axial vibration of a beam element

$$\begin{bmatrix} N_1 \\ N_2 \end{bmatrix} = \begin{bmatrix} a_1 & a_2 \\ a_2 & a_1 \end{bmatrix}\begin{bmatrix} U_1 \\ U_2 \end{bmatrix} \tag{26}$$

where

$$a_1 = EA(1 + i\omega\zeta_k)k_a\cot(k_a)/L, a_2 = -EA(1 + i\omega\zeta_k)k_a\csc(k_a)/L\,. \tag{27}$$

#### 2.5.2. Bending vibration based on Euler-Bernoulli theory

The governing differential equation (Leung, 1993; Paz, 1980; Petyt, 1990) for bending vibration based on Euler-Bernoulli beam theory is given as follows

$$EI\left(1 + \zeta_k\frac{\partial}{\partial t}\right)\frac{\partial^4 w}{\partial x^4} + \rho A\frac{\partial^2 w}{\partial t^2} + c_b\frac{\partial w}{\partial t} = 0 \tag{28}$$

and the natural boundary conditions are given as

$$\begin{aligned} M(x) &= EI\left(1 + \zeta_k\frac{\partial}{\partial t}\right)\frac{\partial^2 w}{\partial x^2} \\ V(x) &= -EI\left(1 + \zeta_k\frac{\partial}{\partial t}\right)\frac{\partial^3 w}{\partial x^3} \end{aligned} \tag{29}$$

where $c_b$ is the velocity-dependent viscous damping coefficient for bending deformation, $EI$ is the bending stiffness of the beam, $I$ is the inertia moment of the beam cross section. By introducing the harmonic vibration assumption $w(x,t) = W(x)e^{i\omega t}$, we have the following characteristic equation

$$\left(D^4 - k_b^4\right)W = 0 \tag{30}$$

where $D = d/d\xi = Ld/dx$ and

$$k_b^4 = \frac{(\rho A\omega^2 - i\omega c_b)L^4}{EI(1+i\omega\zeta_k)} = \frac{\rho A\omega^2 L^4(1-i\zeta_{mb}/\omega)}{EI(1+i\omega\zeta_k)} = \frac{12\rho\omega^2 L^4(1-i\zeta_{mb}/\omega)}{Et^2(1+i\omega\zeta_k)} \tag{31}$$

Therefore, the general solutions of $W(\xi)$ is

$$\begin{aligned} W(\xi) &= c_1\sin(k_b\xi) + c_2\cos(k_b\xi) + c_3\sinh(k_b\xi) + c_4\cosh(k_b\xi) \\ \Theta(\xi) &= c_1k_b\cos(k_b\xi) - c_2k_b\sin(k_b\xi) + c_3k_b\cosh(k_b\xi) + c_4k_b\sinh(k_b\xi) \end{aligned} \tag{32}$$

The displacement and force boundary conditions can be applied as follows

$$\begin{aligned} &W(0) = W_1, \Theta(0) = \Theta_1, W(1) = W_2, \Theta(1) = \Theta_2 \\ &V(0) = -V_1, M(0) = -M_1, V(1) = V_2, M(1) = M_2 \end{aligned} \tag{33}$$

By eliminating the unknowns $c_1, c_2, c_3$ and $c_4$, we have the dynamic stiffness matrix for a Euler-Bernoulli beam element

$$\begin{bmatrix} V_1 \\ M_1 \\ V_2 \\ M_2 \end{bmatrix} = \begin{bmatrix} d_1 & d_2 & d_4 & d_5 \\ & d_3 & -d_5 & d_6 \\ & & d_1 & -d_2 \\ sym & & & d_3 \end{bmatrix} \begin{bmatrix} W_1 \\ \Theta_1 \\ W_2 \\ \Theta_2 \end{bmatrix} \tag{34}$$

where

$$\begin{aligned} d_1 &= R_3(cS + sC)/\delta \\ d_2 &= R_2 sS/\delta \\ d_3 &= R_1(sC - cS)/\delta \\ d_4 &= -R_3(s+S)/\delta \\ d_5 &= R_2(C-c)/\delta \\ d_6 &= R_1(S-s)/\delta \end{aligned} \tag{35}$$

and where

$$\begin{aligned} &R_j = EI(k_b/L)^j \quad j = 1,2,3 \\ s = \sin k_b, \quad &c = \cos k_b, \quad S = \sinh k_b, \quad C = \cosh k_b \\ &\delta = 1 - cC \end{aligned} \tag{36}$$

### 2.5.3. Bending vibration based on Timoshenko theory

The governing differential equation (Leung, 1993) for bending vibration based on Timoshenko beam theory is given as follows

$$\begin{aligned} &kAG\left(1+\zeta_k\frac{\partial}{\partial t}\right)\frac{\partial}{\partial x}\left(\frac{\partial w}{\partial x} - \theta\right) - \rho A\frac{\partial^2 w}{\partial t^2} - c_s\frac{\partial w}{\partial t} = 0 \\ &EI\left(1+\zeta_k\frac{\partial}{\partial t}\right)\frac{\partial^2\theta}{\partial x^2} + kAG\left(1+\zeta_k\frac{\partial}{\partial t}\right)\left(\frac{\partial w}{\partial x} - \theta\right) - \rho I\frac{\partial^2\theta}{\partial t^2} - c_b\frac{\partial\theta}{\partial t} = 0 \end{aligned} \tag{37}$$

where $c_s$ and $c_b$ are the velocity-dependent viscous damping coefficients for both shear and bending deformations, $kAG$ and $EI$ are the shear and bending stiffnesses of the beam, $I$ is the inertia moment of the beam cross section. The natural boundary conditions are given as

$$\begin{aligned} M(x) &= -EI\left(1+\zeta_k\frac{\partial}{\partial t}\right)\frac{\partial\theta}{\partial x} \\ V(x) &= -kAG\left(1+\zeta_k\frac{\partial}{\partial t}\right)\left(\frac{\partial w}{\partial x} - \theta\right) \end{aligned} \tag{38}$$

By introducing the non-dimensional length $\xi = x/L$ and harmonic vibration assumptions $w(x,t) = W(x)e^{i\omega t}$ and $\theta(x,t) = \Theta(x)e^{i\omega t}$, we have the following characteristic equation

$$\left[D^4 + \overline{b}^2\left(r^2+s^2\right)D^2 - \overline{b}^2\left(1 - \overline{b}^2 r^2 s^2\right)\right]H = 0 \tag{39}$$

where $D = \mathrm{d}/\mathrm{d}\xi = L\mathrm{d}/\mathrm{d}x; H = W$ or $\Theta$ and

$$\begin{aligned} \overline{b}^2 &= \frac{(\rho A\omega^2 - i\omega c_s)L^4}{EI(1+i\omega\zeta_k)} = \frac{12\rho\omega^2 L^4(1-i\zeta_{ms}/\omega)}{Et^2(1+i\omega\zeta_k)} \\ r^2 &= \frac{\rho I\omega^2 - i\omega c_b}{(\rho A\omega^2 - i\omega c_s)L^2} = \frac{1}{12}\left(\frac{t}{L}\right)^2\frac{1-i\zeta_{mb}/\omega}{1-i\zeta_{ms}/\omega} \\ s^2 &= \frac{EI(1+i\omega\zeta_k)}{kAG(1+i\omega\zeta_k)L^2} = \frac{(1+\nu)}{6k}\left(\frac{t}{L}\right)^2 \end{aligned} \tag{40}$$

Therefore, the general solutions of $W(\xi)$ and $\Theta(\xi)$ are

$$\begin{aligned} W(\xi) &= A_1\cos\lambda_1\xi + A_2\sin\lambda_1\xi + A_3\cosh\lambda_2\xi + A_4\sinh\lambda_2\xi \\ \Theta(\xi) &= B_1\cos\lambda_1\xi + B_2\sin\lambda_1\xi + B_3\cosh\lambda_2\xi + B_4\sinh\lambda_2\xi \end{aligned} \tag{41}$$

where

$$\left.\begin{matrix}\lambda_1 \\ \lambda_2\end{matrix}\right\} = b\left\{\pm\Delta\Big/2 + \left[\Delta^2\Big/4 + \left(1 - \overline{b}^2 r^2 s^2\right)\Big/\overline{b}^2\right]^{1/2}\right\}^{1/2} \tag{42}$$

with $\Delta = r^2 + s^2$ and

$$B_1 = k_1A_2/L \quad B_2 = -k_1A_1/L \quad B_3 = k_2A_4/L \quad B_4 = k_2A_3/L \tag{43}$$

with

$$k_1 = \left(\lambda_1^2 - \overline{b}^2 s^2\right)\Big/\lambda_1, \quad k_2 = \left(\lambda_2^2 + \overline{b}^2 s^2\right)\Big/\lambda_2 \tag{44}$$

The displacement and force boundary conditions can be applied as follows

$$\begin{aligned} &W(0) = W_1, \Theta(0) = \Theta_1, W(1) = W_2, \Theta(1) = \Theta_2 \\ &V(0) = -V_1, M(0) = -M_1, V(1) = V_2, M(1) = M_2 \end{aligned} \tag{45}$$

By eliminating the unknowns $A_1, A_2, A_3$ and $A_4$, we have the dynamic stiffness matrix for a Timoshenko beam element

$$\begin{bmatrix} V_1 \\ M_1 \\ V_2 \\ M_2 \end{bmatrix} = \begin{bmatrix} d_1 & d_2 & d_4 & d_5 \\ & d_3 & -d_5 & d_6 \\ & & d_1 & -d_2 \\ sym & & & d_3 \end{bmatrix} \begin{bmatrix} W_1 \\ \Theta_1 \\ W_2 \\ \Theta_2 \end{bmatrix} \tag{46}$$

where

$$\begin{aligned} d_1 &= R_3\overline{b}^2(\lambda_2 + \eta\lambda_1)(cS + \eta sC)\Big/(\lambda_1\lambda_2\delta) \\ d_2 &= R_2k_1[(\lambda_1 + \eta\lambda_2)sS - (\lambda_2 - \eta\lambda_1)(1 - cC)]/\delta \\ d_3 &= R_1(\lambda_2 + \eta\lambda_1)(sC - \eta cS)/\delta \\ d_4 &= -R_3\overline{b}^2(\lambda_2 + \eta\lambda_1)(S + \eta s)\Big/(\lambda_1\lambda_2\delta) \\ d_5 &= R_2k_1(\lambda_2 + \eta\lambda_1)(C - c)/\delta \\ d_6 &= R_1(\lambda_2 + \eta\lambda_1)(\eta S - s)/\delta \end{aligned} \tag{47}$$

and where

$$\begin{aligned} &R_j = EI(1+i\omega\zeta_k)/L^j, \quad j = 1,2,3 \\ s = \sin\lambda_1, \quad &c = \cos\lambda_1, \quad S = \sinh\lambda_2, \quad C = \cosh\lambda_2 \\ &\eta = k_1/k_2, \quad \delta = 2\eta(1 - cC) + \left(1 - \eta^2\right)sS \end{aligned} \tag{48}$$

According to Sections 2.3 and 2.4, the elemental matrix of a beam element can be written as

$$\mathbf{K}_d(\omega) = \begin{bmatrix} a_1 & 0 & 0 & a_2 & 0 & 0 \\ 0 & d_1 & d_2 & 0 & d_4 & d_5 \\ 0 & d_2 & d_3 & 0 & -d_5 & d_6 \\ a_2 & 0 & 0 & a_1 & 0 & 0 \\ 0 & d_4 & -d_5 & 0 & d_1 & -d_2 \\ 0 & d_5 & d_6 & 0 & -d_2 & d_3 \end{bmatrix} \tag{49}$$

The subscript $d$ in the above equation denotes the fact that the stiffness matrix is obtained using the shape functions satisfying the equation of dynamic motion.

## 3. General derivation of stretching enriched in-plane elastic moduli

Dynamic behaviour of the overall lattice structure depends on the frequency-dependent deformation characteristics of the constituent individual beams. A representative depiction of the constituent beam elements is shown in Fig. 1(b–c). Vibration mode of these constituent members is shown symbolically, wherein the vibrating beams would undergo deformation under applied external loads. The rule of deformation in such cases would be different from the static condition. This leads to a different value of effective elastic moduli of the lattice material from conventional static values. In the previous section, the stiffness matrix of a beam element is given considering the static and dynamic equilibrium incorporating the bending, shear and axial deformations. The objective of this section is to express equivalent in-plane elastic moduli of the lattice in terms of the stiffness matrix elements of the beams using the unit cell approach. For the case of equivalent static properties of the lattice, we refer to well-known references by Gibson and Ashby (1999) and Masters and Evans (1996). For the sake of generality, we consider the dynamic equilibrium of the unit cell under a different stress condition. A general notation of the frequency-dependent stiffness matrix $\mathbf{K}(\omega)$ is employed here.

### 3.1. The longitudinal Young's modulus $E_1$ and the Poisson's ratio $\nu_{12}$

A uniform harmonic stress $\bar{\sigma}_1 = \sigma_1(\omega)e^{i\omega t}$ is applied to the unit cell in direction-1 (refer to Fig. 4) for deriving the expression of longitudinal Young's modulus. This results in an harmonic force $\bar{P} = P(\omega)e^{i\omega t}$ being applied at point A (and B) on the unit cell. We consider the steady-state condition for the dynamic equilibrium and express free-body diagram for a given frequency.

The deformation of the unit cell is symmetric about the OC line. The amplitude of the force $P$ acting on point A for a given frequency ω is given by

$$P(\omega) = \sigma_1(\omega)b(h + l\sin\theta) \tag{50}$$

Considering $\eta_A(\omega)$ and $\gamma_A(\omega)$ as deformations transverse and along the inclined member AO, we have

$$\eta_A(\omega) = \frac{P(\omega)\sin\theta}{K_{55}(\omega)} \quad \text{and} \quad \gamma_A(\omega) = \frac{P(\omega)\cos\theta}{K_{44}(\omega)} \tag{51}$$

Here $K_{55}(\omega)$ and $K_{44}(\omega)$ are elements of the stiffness matrix of the inclined member AO of length $l$. Due to the presence of damping, $K_{55}(\omega)$ and $K_{44}(\omega)$ are in general complex valued functions of the frequency parameter ω. As a result, the deformations $\eta_A(\omega)$ and $\gamma_A(\omega)$ are complex valued functions of ω. The total dynamic deflection in the 1-direction is therefore

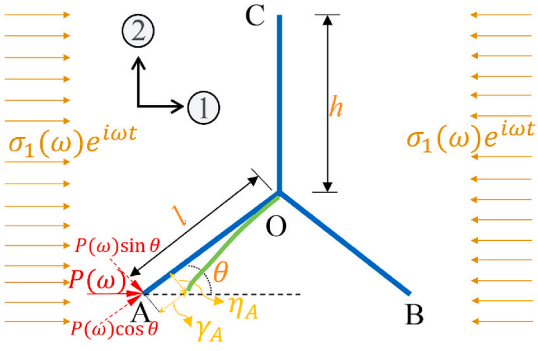


**Fig. 4.** Dynamic equilibrium and deformation patterns of the unit cell under the application of a harmonic stress field $\bar{\sigma}_1 = \sigma_1(\omega)e^{i\omega t}$ applied in the 1-direction. This configuration is used for the derivation of the longitudinal Young's modulus $E_1(\omega)$ and the Poisson's ratio $\nu_{12}(\omega)$.

$$\begin{aligned}\delta_1(\omega) &= \eta_A(\omega)\sin\theta + \gamma_A(\omega)\cos\theta = P(\omega)\left(\frac{\sin^2\theta}{K_{55}(\omega)} + \frac{\cos^2\theta}{K_{44}(\omega)}\right)\\ &= \frac{P\sin^2\theta}{K_{55}(\omega)}\left(1 + \cot^2\theta\frac{K_{55}(\omega)}{K_{44}(\omega)}\right)\end{aligned} \tag{52}$$

The strain the 1-direction is obtained as

$$\varepsilon_1(\omega) = \frac{\delta_1(\omega)}{l\cos\theta} = \frac{\sigma_1(\omega)b(h/l + \sin\theta)\sin^2\theta}{K_{55}(\omega)\cos\theta}\left(1 + \cot^2\theta\frac{K_{55}(\omega)}{K_{44}(\omega)}\right) \tag{53}$$

Using this, the Young's modulus in 1-direction is obtained in terms of the elements of the stiffness matrix as

$$E_1(\omega) = \frac{\sigma_1(\omega)}{\varepsilon_1(\omega)} = \frac{K_{55}(\omega)\cos\theta}{b(h/l + \sin\theta)\sin^2\theta\left(1 + \cot^2\theta\frac{K_{55}(\omega)}{K_{44}(\omega)}\right)} \tag{54}$$

To obtain the Poisson's ratio $\nu_{12}$, we need to obtain the strain in the direction 2 for applied stress in the 1-direction. Using the expressions of the deformations in Eq. (51), we obtain total deflection in the 2-direction as

$$\begin{aligned}-\delta_2(\omega) &= \eta_A(\omega)\cos\theta - \gamma_A(\omega)\sin\theta = P(\omega)\left(\frac{\sin\theta\cos\theta}{K_{55}(\omega)} - \frac{\sin\theta\cos\theta}{K_{44}(\omega)}\right)\\ &= \frac{P(\omega)\sin\theta\cos\theta}{K_{55}(\omega)}\left(1 - \frac{K_{55}(\omega)}{K_{44}(\omega)}\right)\end{aligned} \tag{55}$$

The total strain in the 2-direction is

$$-\varepsilon_2(\omega) = \frac{\delta_2(\omega)}{h + l\sin\theta} = \frac{\sigma_1(\omega)b\sin\theta\cos\theta}{K_{55}(\omega)}\left(1 - \frac{K_{55}(\omega)}{K_{44}(\omega)}\right) \tag{56}$$

Using the expressions of the strains in directions 1 and 2 given by Eqs. (53) and (56), we obtain the Poisson's ratio $\nu_{12}$

$$\nu_{12}(\omega) = -\frac{\varepsilon_2(\omega)}{\varepsilon_1(\omega)} = \frac{\cos^2\theta\left(1 - \frac{K_{55}(\omega)}{K_{44}(\omega)}\right)}{(h/l + \sin\theta)\sin\theta\left(1 + \cot^2\theta\frac{K_{55}(\omega)}{K_{44}(\omega)}\right)} \tag{57}$$

From equations (54) and (57), it can be observed that only two coefficients of the $6 \times 6$ element stiffness matrix of the inclined member, namely, $K_{55}(\omega)$ and $K_{44}(\omega)$, contribute towards the value of $E_1$ and $\nu_{12}$, which in general are complex valued functions of the frequency ω due to the presence of damping.

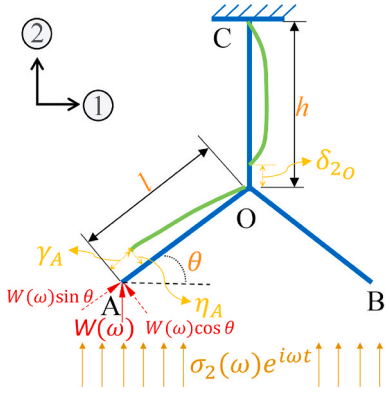


**Fig. 5.** Dynamic equilibrium and deformation patterns of the unit cell under application of a harmonic stress field $\bar{\sigma}_2 = \sigma_2(\omega)e^{i\omega t}$ applied in the 2-direction. This configuration is used for the derivation of the transverse Young's modulus $E_2(\omega)$ and the Poisson's ratio $\nu_{21}(\omega)$.

### 3.2. The transverse Young's modulus $E_2$ and the Poisson's ratio $\nu_{21}$

For deriving the expression of transverse Young's modulus and Poisson's ratio $\nu_{21}$, a uniform harmonic stress $\overline{\sigma}_2 = \sigma_2(\omega)e^{i\omega t}$ is applied to the unit cell in direction-2 as shown in Fig. 5.

From the free-body diagram depicting the dynamic equilibrium at the steady state condition, we deduce that the deformation of the unit cell is symmetric about the OC line. It addition, the point O has no deflection in the 1-direction. Therefore, it is sufficient to consider the deflection of point A or B with respect to point C under the applied stress. Considering point A, the harmonic stress results in a harmonic vertical force $\overline{W} = W(\omega)e^{i\omega t}$ for a given frequency ω. The amplitude of this vertical force is given by

$$W(\omega) = \sigma_2(\omega) bl\cos\theta \tag{58}$$

Considering $\eta_A$ and $\gamma_A$ as deformations transverse and along the inclined member AO, we have

$$\eta_A(\omega) = \frac{W(\omega)\cos\theta}{K_{55}(\omega)} \quad \text{and} \quad \gamma_A(\omega) = \frac{W(\omega)\sin\theta}{K_{44}(\omega)} \tag{59}$$

Here $K_{55}$ and $K_{44}$ are elements of the stiffness matrix of the member AO. The deflection in the 2-direction is therefore

$$\begin{aligned}\delta_{2_{AO}}(\omega) &= \eta_A(\omega)\cos\theta + \gamma_A(\omega)\sin\theta = W(\omega)\left(\frac{\cos^2\theta}{K_{55}(\omega)} + \frac{\sin^2\theta}{K_{44}(\omega)}\right) \\ &= \frac{W(\omega)\cos^2\theta}{K_{55}(\omega)}\left(1 + \tan^2\theta\frac{K_{55}(\omega)}{K_{44}(\omega)}\right)\end{aligned} \tag{60}$$

The total force acting in the 2-direction at point O is $2W$. Therefore, the displacement of point O in the 2-direction arising from the axial deformation of the vertical member OC is

$$\delta_{2_O}(\omega) = \frac{2W(\omega)}{K_{44}^{(h)}(\omega)} \tag{61}$$

Here $(\bullet)^{(h)}$ corresponds to the properties arising from the vertical member OC of length $h$. The total deflection in the 2-direction is therefore

$$\delta_2(\omega) = \delta_{2_{AO}}(\omega) + \delta_{2_O}(\omega) = \frac{W(\omega)\cos^2\theta}{K_{55}(\omega)}\left(1 + \tan^2\theta\frac{K_{55}(\omega)}{K_{44}(\omega)} + 2\sec^2\theta\frac{K_{55}(\omega)}{K_{44}^{(h)}(\omega)}\right) \tag{62}$$

The strain the 2-direction is obtained as

$$\varepsilon_2(\omega) = \frac{\delta_2(\omega)}{h + l\sin\theta} = \frac{\sigma_2(\omega)b\cos^3\theta}{K_{55}(\omega)(h/l + \sin\theta)}\left(1 + \tan^2\theta\frac{K_{55}(\omega)}{K_{44}(\omega)} + 2\sec^2\theta\frac{K_{55}(\omega)}{K_{44}^{(h)}(\omega)}\right) \tag{63}$$

Using this, the Young's modulus in 1-direction is obtained in terms of the elements of the stiffness matrix as

$$E_2(\omega) = \frac{\sigma_2(\omega)}{\varepsilon_2(\omega)} = \frac{K_{55}(\omega)(h/l + \sin\theta)}{b\cos^3\theta\left(1 + \tan^2\theta\frac{K_{55}(\omega)}{K_{44}(\omega)} + 2\sec^2\theta\frac{K_{55}(\omega)}{K_{44}^{(h)}(\omega)}\right)} \tag{64}$$

To obtain the Poisson's ratio $\nu_{21}$, we need to obtain the strain in the direction 1 due to the applied stress in the 2-direction. Using the expressions of the deformations in Eq. (59), we obtain total deflection in the 1-direction as

$$\begin{aligned}\delta_1(\omega) &= \gamma_A(\omega)\cos\theta - \eta_A(\omega)\sin\theta = -W(\omega)\left(\frac{\sin\theta\cos\theta}{K_{55}(\omega)} - \frac{\sin\theta\cos\theta}{K_{44}(\omega)}\right) \\ &= -\frac{W(\omega)\sin\theta\cos\theta}{K_{55}(\omega)}\left(1 - \frac{K_{55}(\omega)}{K_{44}(\omega)}\right)\end{aligned} \tag{65}$$

The total strain in the 1-direction is

$$\varepsilon_1(\omega) = \frac{\delta_1(\omega)}{l\cos\theta} = -\frac{\sigma_2(\omega)b\sin\theta}{lK_{55}(\omega)}\left(1 - \frac{K_{55}(\omega)}{K_{44}(\omega)}\right) \tag{66}$$

Using the expressions of the strains in directions 1 and 2 given by Eqs. (53) and (56), we obtain the Poisson's ratio $\nu_{21}$

$$\nu_{21}(\omega) = -\frac{\varepsilon_1(\omega)}{\varepsilon_2(\omega)} = \frac{(h/l + \sin\theta)\sin\theta\left(1 - \frac{K_{55}(\omega)}{K_{44}(\omega)}\right)}{\cos^2\theta\left(1 + \tan^2\theta\frac{K_{55}(\omega)}{K_{44}(\omega)} + 2\sec^2\theta\frac{K_{55}(\omega)}{K_{44}^{(h)}(\omega)}\right)} \tag{67}$$

From equations (64) and (57), it can be observed that only two coefficients of the $6 \times 6$ element stiffness matrix of the inclined member and one coefficients of the $6 \times 6$ element stiffness matrix of vertical member, namely, $K_{55}(\omega)$, $K_{44}(\omega)$ and $K_{44}^{(h)}(\omega)$, contribute towards the value of $E_2$ and $\nu_{21}$. Like the previous case, in general the Young's moduli as well as the Poisson's ratio are complex valued functions of the frequency ω due to the presence of damping.

The proposed expressions of the general frequency dependent elastic moduli also conform the reciprocal theorem

$$E_1(\omega)\nu_{21}(\omega) = E_2(\omega)\nu_{12}(\omega) = \frac{K_{55}(\omega)}{b\sin\theta\left(1 + \cot^2\theta\frac{K_{55}(\omega)}{K_{44}(\omega)}\right)}\frac{\left(1 - \frac{K_{55}(\omega)}{K_{44}(\omega)}\right)}{\cos\theta\left(1 + \tan^2\theta\frac{K_{55}(\omega)}{K_{44}(\omega)} + 2\sec^2\theta\frac{K_{55}(\omega)}{K_{44}^{(h)}(\omega)}\right)} \tag{68}$$

### 3.3. Shear modulus $G_{12}$

The derivation of the shear modulus $G_{12}(\omega)$ requires the superpositions strain contributions arising from bending and axial deformations. In Fig. 6, the consideration of both the cases are depicted. For deriving the bending contributions, considering the deformation of the adjacent cells, it can be deduced that the mid point of the vertical member will only have a deformation in the 1-direction due to shear. Therefore, in Fig. 6(a) we consider the unit cell with the vertical member with length $h/2$ and a slant member with the usual length $l$. The points A and O will not have any relative movement due to symmetrical structure. The shear deflection $\gamma_D$ due to bending consists of two components, namely, bending deflection of the member OD and its deflection due to rotation of joint O arising from the bending of the slant members.

It can be noted here that the elements of the dynamic stiffness matrix (refer to equation (49)) will be different for the vertical member and the slant member due to their different lengths. Using the stiffness components of the dynamic stiffness matrix with length $h/2$, the bending deformation of point D with respect to point O in direction the 1 can be obtained as

$$\eta_D(\omega) = \frac{F_1(\omega)}{\left(K_{55}^{(h/2)}(\omega) - \frac{K_{56}^{(h/2)}(\omega)K_{65}^{(h/2)}(\omega)}{K_{66}^{(h/2)}(\omega)}\right)} = \frac{F_1(\omega)K_{66}^{(h/2)}(\omega)}{\left(K_{55}^{(h/2)}(\omega)K_{66}^{(h/2)}(\omega) - \left(K_{56}^{(h/2)}(\omega)\right)^2\right)} \tag{69}$$

Here

$$F_1(\omega) = 2\tau(\omega)lb\cos\theta \tag{70}$$

and we make use of the symmetry of the elements of the dynamic stiffness matrix. Here $(\cdot)^{(h/2)}$ corresponds to the properties arising from the vertical member OD of length $h/2$ as shown in Fig. 6(a).

From the diagram in Fig. 6(a), the moment acting on point O is obtained as

$$M(\omega) = \frac{F_1(\omega)}{2} \times \frac{h}{2} = \frac{F_1(\omega)h}{4} \tag{71}$$

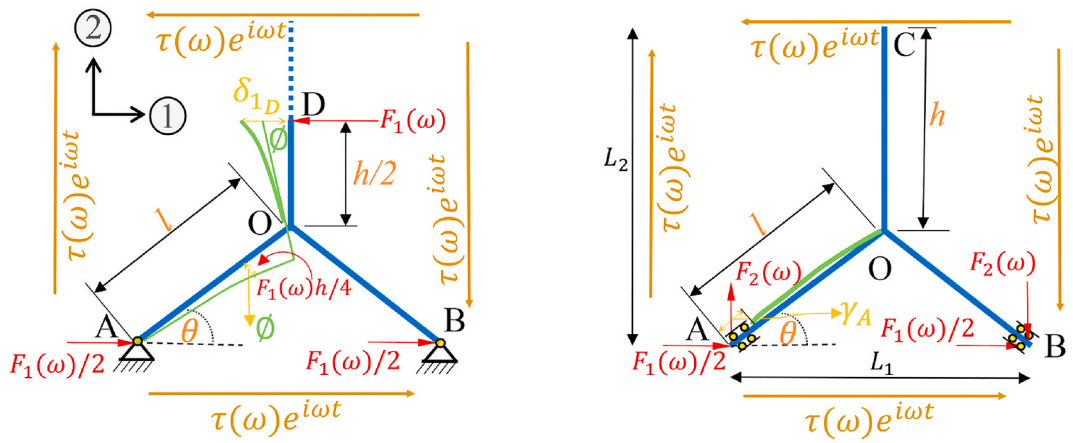


(a) Shear strain due to bending (b) Shear strain due to axial deformation

**Fig. 6.** Dynamic equilibrium and patterns patters of the unit cell under the application of the harmonic shear stress field $\bar{\tau} = \tau(\omega)e^{i\omega t}$. These configurations are used for the derivation of the shear modulus $G_{12}(\omega)$.

On the basis of the degrees of freedom as denoted in Fig. 3, deflection of the end O with respect to the end A due to application of moment $M$ at the end O is given as

$$\delta_r(\omega) = \frac{M(\omega)}{-K_{65}(\omega)} \tag{72}$$

Here $K_{65}$ is the stiffness element corresponding to the slant member and the negative arise due to the direction of the rotation as given in Fig. 3. Thus the rotation of joint O can be expressed as

$$\varphi(\omega) = \frac{\delta_r(\omega)}{l} = -\frac{F_1(\omega)h}{4lK_{65}(\omega)} \tag{73}$$

Shear deformation in the 1-direction due to bending at point D under the application of shear stress $\tau$ can be expressed as

$$\begin{aligned}\delta_{1_D}(\omega) &= 2\left(\varphi(\omega)\frac{h}{2} + \eta_D(\omega)\right)\\ &= -\frac{F_1(\omega)h^2}{4lK_{65}(\omega)} + \frac{2F_1(\omega)K_{66}^{(h/2)}(\omega)}{\left(K_{55}^{(h/2)}(\omega)K_{66}^{(h/2)}(\omega) - \left(K_{56}^{(h/2)}(\omega)\right)^2\right)}\end{aligned} \tag{74}$$

The factor 2 in the above expression arises due to the consideration of two units shown in Fig. 6(a) to capture the total shear deformation by representing a complete unit cell that can create the entire lattice structure on tessellation.

To obtain the shear deformation due to axial stretching deformation, we consider the forcing $F_2(\omega)$ in the 2-direction as

$$F_2(\omega) = \tau(\omega)b(h + l\sin\theta) \tag{75}$$

Due to the symmetry of the unit cell as depicted in Fig. 6(b), the deformation in the 1-direction of member AO and BO will be the same. On the other hand, the amplitude of the deformation in the 2-direction of member AO and BO will be the same, but in the opposite direction. There is no axial deformation in the vertical member OC. It is therefore sufficient to consider only one inclined element in our calculation. The lengths of the unit cell in Fig. 6(b) in the 1 and 2 directions are given by

$$L_1 = 2l\cos\theta \tag{76}$$

and $$L_2 = (h + l\sin\theta) \tag{77}$$

Total force acting in the axial direction of AO is given by

$$F_{\mathrm{AO}}(\omega) = F_1 \,/\, 2\cos\theta + F_2\sin\theta = \tau(\omega)lb\left(\cos^2\theta + (h/l + \sin\theta)\sin\theta\right) \tag{78}$$

The axial deformation of point A is therefore

$$\gamma_A(\omega) = \frac{F_{\mathrm{AO}}(\omega)}{K_{44}(\omega)} \tag{79}$$

Using this, the deformation in the 1 and 2 directions are obtained as

$$\delta_{1_A}(\omega) = \gamma_A(\omega)\cos\theta = \frac{\tau(\omega)lb}{K_{44}(\omega)}\left(\cos^2\theta + (h/l + \sin\theta)\sin\theta\right)\cos\theta \tag{80}$$

$$\delta_{2_A}(\omega) = \gamma_A(\omega)\sin\theta = \frac{\tau(\omega)lb}{K_{44}(\omega)}\left(\cos^2\theta + (h/l + \sin\theta)\sin\theta\right)\sin\theta \tag{81}$$

The total shear strain arising due to bending and axial deformation is given by

$$\gamma(\omega) = \frac{\delta_{1_A}(\omega) + \delta_{1_D}(\omega)}{L_2} + \frac{2\delta_{2_A}(\omega)}{L_1} = \frac{\delta_{1_A}(\omega) + \delta_{1_D}(\omega)}{h + l\sin\theta} + \frac{2\delta_{2_A}(\omega)}{2l\cos\theta} \tag{82}$$

$$= \underbrace{\frac{\delta_{1_D}(\omega)}{h + l\sin\theta}}_{\gamma_b(\omega)} + \underbrace{\frac{\delta_{1_A}(\omega)}{h + l\sin\theta} + \frac{\delta_{2_A}(\omega)}{l\cos\theta}}_{\gamma_s(\omega)} \tag{83}$$

Here $\gamma_b(\omega)$ and $\gamma_s(\omega)$ are respectively the bending and stretching components of the total shear strain. Using Eq. (74) we obtain the bending component of the shear strain as

$$\begin{aligned}\gamma_b(\omega) &= \frac{\delta_{1_D}(\omega)}{(h + l\sin\theta)}\\ &= \frac{F_1(\omega)}{(h + l\sin\theta)}\left(-\frac{h^2}{4lK_{65}(\omega)} + \frac{2K_{66}^{(h/2)}(\omega)}{\left(K_{55}^{(h/2)}(\omega)K_{66}^{(h/2)}(\omega) - \left(K_{56}^{(h/2)}(\omega)\right)^2\right)}\right)\\ &= \frac{2\tau(\omega)lb\cos\theta}{(h + l\sin\theta)}\left(-\frac{h^2}{4lK_{65}(\omega)} + \frac{2K_{66}^{(h/2)}(\omega)}{\left(K_{55}^{(h/2)}(\omega)K_{66}^{(h/2)}(\omega) - \left(K_{56}^{(h/2)}(\omega)\right)^2\right)}\right)\\ &= \frac{\tau(\omega)b\cos\theta}{(h/l + \sin\theta)}\left(-\frac{h^2}{2lK_{65}(\omega)} + \frac{4K_{66}^{(h/2)}(\omega)}{\left(K_{55}^{(h/2)}(\omega)K_{66}^{(h/2)}(\omega) - \left(K_{56}^{(h/2)}(\omega)\right)^2\right)}\right)\end{aligned} \tag{84}$$

The stretching component of the shear strain can be simplified as

$$\gamma_s(\omega) = \frac{\delta_{1_A}(\omega)}{h + l\sin\theta} + \frac{\delta_{2_A}(\omega)}{l\cos\theta} \tag{85}$$

$$= \frac{\tau(\omega) lb}{K_{44}(\omega)} \left(\cos^2\theta + (h/l + \sin\theta)\sin\theta\right) \left(\frac{\cos\theta}{h + l\sin\theta} + \frac{\sin\theta}{l\cos\theta}\right) \tag{86}$$

$$= \frac{\tau(\omega) b}{K_{44}(\omega)} \frac{\left(\cos^2\theta + (h/l + \sin\theta)\sin\theta\right)^2}{\cos\theta(h/l + \sin\theta)} \tag{87}$$

Substituting the expressions of both the shear strains, the modulus can be obtained as

$$\begin{aligned} G_{12}(\omega) &= \frac{\tau(\omega)}{\gamma(\omega)} = \frac{\tau(\omega)}{\gamma_b(\omega) + \gamma_s(\omega)} \\ &= \frac{1}{\frac{b\cos\theta}{(h/l+\sin\theta)}\left(-\frac{h^2}{2lK_{65}(\omega)} + \frac{4K_{66}^{(h/2)}(\omega)}{\left(K_{55}^{(h/2)}(\omega)K_{66}^{(h/2)}(\omega) - \left(K_{56}^{(h/2)}(\omega)\right)^2\right)}\right) + \frac{b}{K_{44}(\omega)}\frac{\left(\cos^2\theta + (h/l+\sin\theta)\sin\theta\right)^2}{\cos\theta(h/l+\sin\theta)}} \\ &= \frac{(h/l+\sin\theta)}{b\cos\theta} \frac{1}{\left(-\frac{h^2}{2lK_{65}(\omega)} + \frac{4K_{66}^{(h/2)}(\omega)}{\left(K_{55}^{(h/2)}(\omega)K_{66}^{(h/2)}(\omega) - \left(K_{56}^{(h/2)}(\omega)\right)^2\right)} + \frac{(\cos\theta + (h/l+\sin\theta)\tan\theta)^2}{K_{44}(\omega)}\right)} \end{aligned} \tag{88}$$

From equation (88) it can be observed that in total five elements of two different stiffness matrices contribute to the shear modulus. They include two coefficients of the $6 \times 6$ element stiffness matrix of the inclined member, namely, $K_{65}(\omega)$, $K_{44}(\omega)$. Additionally three elements of the stiffness matrix of the vertical member with half the length, namely, $K_{55}^{(h/2)}(\omega)$, $K_{56}^{(h/2)}(\omega)$ and $K_{66}^{(h/2)}(\omega)$ contribute to the shear modulus. Like the Youngs moduli, in general the shear modulus is a complex valued function of the frequency ω due to the presence of damping.

## 4. Analysis of the special cases

In the previous section, the expressions of five quantities characterising the effective in-plane elastic properties of 2D cellular materials have been derived in terms of the stiffness element of a beam. In total six cases arise depending on what form of the stiffness matrix is employed in the general expressions of the elastic moduli. They include static finite element, dynamic finite element and dynamic stiffness considering Euler-Bernoulli and Timoshenko beam theory. In this section we consider these cases separately and derive explicit closed-form expressions of the $E_1$, $E_2$, $\nu_{12}$ , $\nu_{21}$ and $G_{12}$. A pictorial representation of the special cases and the mapping of their derivation from the more general cases (in terms of the applicability in higher frequency range and thicker

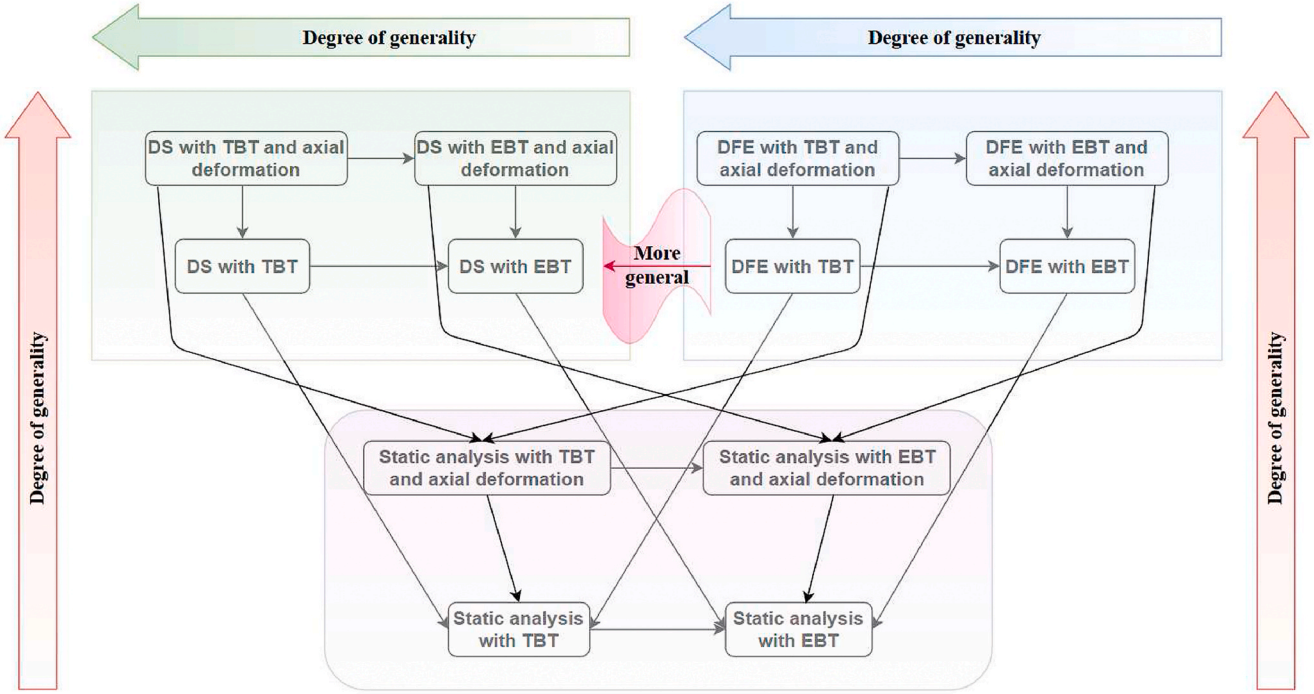


**Fig. 7.** Generality-map of the proposed analytical framework in terms of the applicability in higher frequency band (note that the static case essentially corresponds to zero frequency) and the constraint of cell-wall thickness by considering bending, shear and axial deformation in the formulation. Here DS, DFE, TBT and EBT represent dynamic stiffness, dynamic finite element, Timoshenko beam theory and Euler-Bernoulli beam theory, respectively. The two blocks at the top represent dynamic analyses, while the block at the bottom covers static analysis. It may be noted that, in general, the dynamic analysis using dynamic stiffness approach (the bock at the left-top) is capable of capturing the system behaviour better than the dynamic finite element approach (the bock at the right-top) at higher frequencies.

cell walls) is provided in Fig. 7. It can be noted that the comparison of analytical expressions corresponding to different special cases with available literature provides an exact way of validating the proposed formulation in this article. Considering only the static deformation with Euler-Bernoulli beam theory and ignoring the stretching deformation, the equivalent elastic moduli of hexagonal cellular materials can be obtained as (Gibson and Ashby, 1999)

$$E_{1_{\mathrm{GA}}} = E\alpha^3 \frac{\cos\theta}{(\beta+\sin\theta)\sin^2\theta} \tag{89}$$

$$E_{2_{\mathrm{GA}}} = E\alpha^3 \frac{(\beta+\sin\theta)}{\cos^3\theta} \tag{90}$$

$$\nu_{12_{\mathrm{GA}}} = \frac{\cos^2\theta}{(\beta+\sin\theta)\sin\theta} \tag{91}$$

$$\nu_{21_{\mathrm{GA}}} = \frac{(\beta+\sin\theta)\sin\theta}{\cos^2\theta} \tag{92}$$

$$G_{12_{\mathrm{GA}}} = E\alpha^3 \frac{(\beta+\sin\theta)}{\beta^2(1+2\beta)\cos\theta} \tag{93}$$

Here the α and β are geometric non-dimensional ratios given by

$$\alpha = \frac{t}{l} \tag{94}$$

and

$$\beta = \frac{h}{l} \tag{95}$$

We want to explore the relationships with the expressions proposed here with the above classical expressions. To this end from Eqs. ((54), (57), (64), (67) and (88) and Eq. (93) we obtain the ratios

$$\frac{E_1(\omega)}{E_{1_{\mathrm{GA}}}} = \frac{K_{55}(\omega)}{Eb\alpha^3} \frac{1}{\left(1+\cot^2\theta\frac{K_{55}(\omega)}{K_{44}(\omega)}\right)} \tag{96}$$

$$\frac{E_2(\omega)}{E_{2_{\mathrm{GA}}}} = \frac{K_{55}(\omega)}{Eb\alpha^3} \frac{1}{\left(1+\tan^2\theta\frac{K_{55}(\omega)}{K_{44}(\omega)}+2\sec^2\theta\frac{K_{55}(\omega)}{K_{44}^{(h)}(\omega)}\right)} \tag{97}$$

$$\frac{\nu_{12}(\omega)}{\nu_{12_{\mathrm{GA}}}} = \frac{\left(1-\frac{K_{55}(\omega)}{K_{44}(\omega)}\right)}{\left(1+\cot^2\theta\frac{K_{55}(\omega)}{K_{44}(\omega)}\right)} \tag{98}$$

$$\frac{\nu_{21}(\omega)}{\nu_{21_{\mathrm{GA}}}} = \frac{\left(1-\frac{K_{55}(\omega)}{K_{44}(\omega)}\right)}{\left(1+\tan^2\theta\frac{K_{55}(\omega)}{K_{44}(\omega)}+2\sec^2\theta\frac{K_{55}(\omega)}{K_{44}^{(h)}(\omega)}\right)} \tag{99}$$

$$\frac{G_{12}(\omega)}{G_{12_{\mathrm{GA}}}} = \frac{1}{Eb\alpha^3} \frac{\beta^2(1+2\beta)}{\left(-\frac{h^2}{2lK_{65}(\omega)}+\frac{4K_{66}^{(h/2)}(\omega)}{\left(K_{55}^{(h/2)}(\omega)K_{66}^{(h/2)}(\omega)-\left(K_{56}^{(h/2)}(\omega)\right)^2\right)}+\frac{(\cos\theta+(\beta+\sin\theta)\tan\theta)^2}{K_{44}(\omega)}\right)} \tag{100}$$

Next six special cases are discussed in details in the order of increasing degree of generality and fidelity.

### 4.1. Static elastic moduli with Euler-Bernoulli beam theory

Using the static Euler-Bernoulli beam theory, the element stiffness matrix is obtained in Eq. (6) ignoring the shear deformation. From the derivations in Subsection 3.1 and Subsection 3.2, it can be observed that two coefficients of the $6\times 6$ element stiffness matrix of the inclined member and one coefficients of the $6\times 6$ element stiffness matrix of vertical member, namely, $K_{55}(\omega)$, $K_{44}(\omega)$ and $K_{44}^{(h)}(\omega)$, are necessary to obtain $E_1$, $E_2$ $\nu_{12}$ and $\nu_{21}$. Using the expressions of moment of inertia and the cross-sectional area in Eqs. (10) and (11), the stiffness coefficients are given by

$$K_{55} = \frac{12EI}{l^3} = Eb\alpha^3, K_{44} = \frac{EA}{l} = Eb\alpha \quad \text{and} \quad K_{44}^{(h)} = \frac{EA}{h} = \frac{Ebt}{h} = \frac{Eb\alpha}{\beta} \tag{101}$$

Using these, we obtain the ratios

$$\frac{K_{55}}{K_{44}} = \alpha^2 \quad \text{and} \quad \frac{K_{55}}{K_{44}^{(h)}} = \alpha^2\beta \tag{102}$$

When the static Euler-Bernoulli beam stiffness elements are used, the equivalent elastic properties are not functions of the frequency. Therefore, omitting the frequency dependence, from Eqs. ((54), (57), (64) and (67) we have

$$E_1 = \frac{K_{55}\cos\theta}{b(\beta+\sin\theta)\sin^2\theta\left(1+\cot^2\theta\frac{K_{55}}{K_{44}}\right)} = \frac{E\alpha^3\cos\theta}{(\beta+\sin\theta)\left(\sin^2\theta+\alpha^2\cos^2\theta\right)} \tag{103}$$

$$E_2 = \frac{K_{55}(\beta+\sin\theta)}{b\cos^3\theta\left(1+\tan^2\theta\frac{K_{55}}{K_{44}}+2\sec^2\theta\frac{K_{55}}{K_{44}^{(h)}}\right)} = \frac{E\alpha^3(\beta+\sin\theta)}{(1-\alpha^2)\cos^3\theta+\alpha^2(2\beta+1)\cos\theta} \tag{104}$$

$$\nu_{12} = \frac{\cos^2\theta\left(1-\frac{K_{55}}{K_{44}}\right)}{(\beta+\sin\theta)\sin\theta\left(1+\cot^2\theta\frac{K_{55}}{K_{44}}\right)} = \frac{\cos^2\theta(1-\alpha^2)}{(\beta+\sin\theta)\sin\theta(1+\alpha^2\cot^2\theta)} \tag{105}$$

$$\nu_{21} = \frac{(\beta+\sin\theta)\sin\theta\left(1-\frac{K_{55}(\omega)}{K_{44}}\right)}{\cos^2\theta\left(1+\tan^2\theta\frac{K_{55}}{K_{44}}+2\sec^2\theta\frac{K_{55}}{K_{44}^{(h)}}\right)} = \frac{(\beta+\sin\theta)\sin\theta(1-\alpha^2)}{(1-\alpha^2)\cos^2\theta+\alpha^2(2\beta+1)} \tag{106}$$

For the shear modulus, five elements from two different stiffness matrices are necessary. They are two coefficients of the $6\times 6$ element stiffness matrix of the inclined member, namely, $K_{65}$, $K_{44}$ as in Eq. (101) with $K_{65} = -6\frac{EI}{l^2} = -1/2\,\frac{Ebt^3}{l^2}$. We also need three elements of the stiffness matrix of the vertical member with half the length given by

$$K_{55}^{(h/2)} = \frac{12EI}{(h/2)^3} = \frac{8Ebt^3}{h^3}, K_{56}^{(h/2)} = -\frac{6EI}{(h/2)^2} = -\frac{2Ebt^3}{h^2} \text{ and } K_{66}^{(h/2)} = \frac{4EI}{(h/2)} = \frac{2Ebt^3}{3h} \tag{107}$$

Using these expressions we obtain

$$G_{12} = \frac{(\beta+\sin\theta)}{b\cos\theta} \frac{1}{\left(-\frac{h^2}{2lK_{65}}+\frac{4K_{66}^{(h/2)}}{\left(K_{55}^{(h/2)}K_{66}^{(h/2)}-\left(K_{56}^{(h/2)}\right)^2\right)}+\frac{(\cos\theta+(\beta+\sin\theta)\tan\theta)^2}{K_{44}}\right)} = \frac{E\alpha^3(\beta+\sin\theta)}{\left(\beta^2(1+2\beta)+\alpha^2(\cos\theta+(\beta+\sin\theta)\tan\theta)^2\right)\cos\theta} \tag{108}$$

Substituting $\alpha^2 = 0$ the equations derived here exactly reduce to the corresponding classical expressions in Eqs. (89)–(93) (Gibson and Ashby, 1999) (i.e., the case of considering only the bending deformation).

For a regular lattice $\theta = \frac{\pi}{6}$ and $\beta = \frac{h}{l} = 1$. Substituting these in Eqs. (103)–(106) and (108) we have

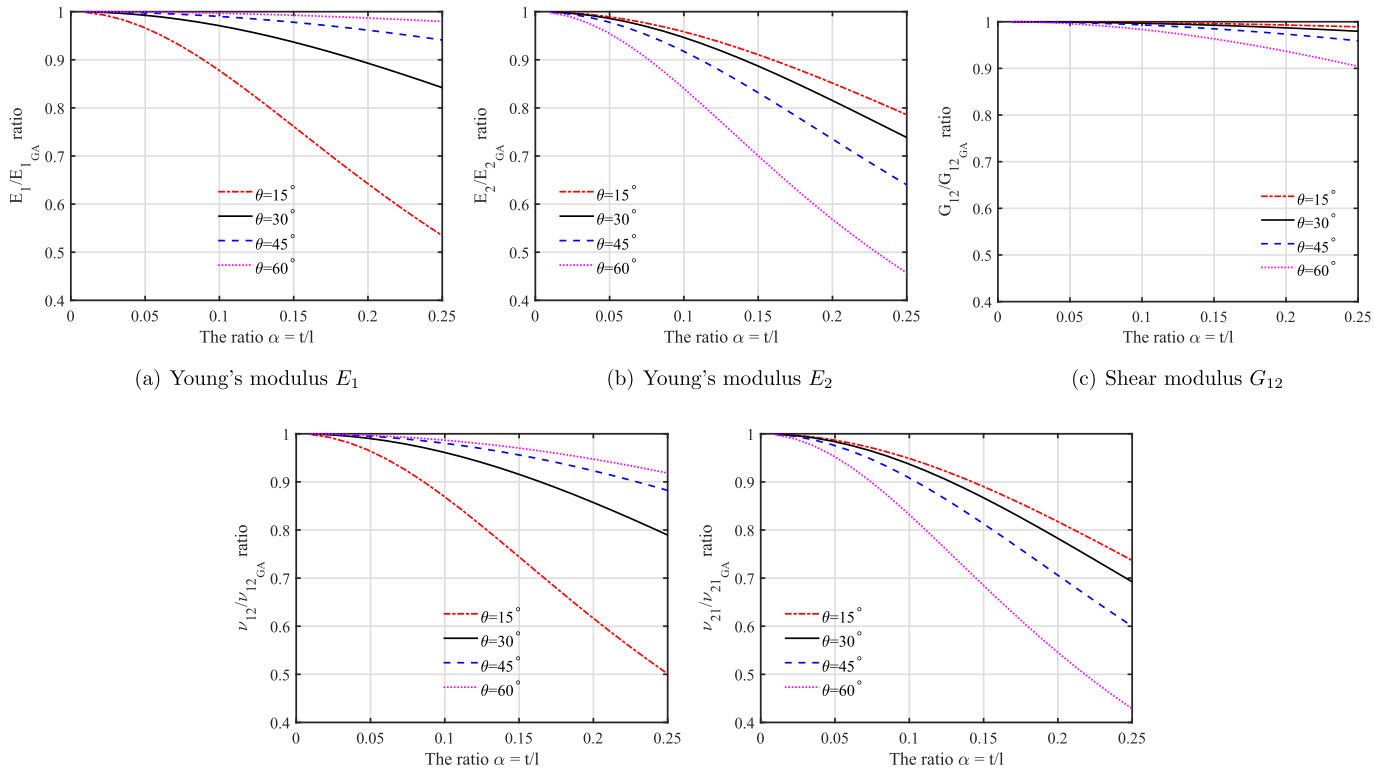


(a) Young's modulus $E_1$ (b) Young's modulus $E_2$ (c) Shear modulus $G_{12}$

(d) Poisson's ratio $\nu_{12}$ (e) Poisson's ratio $\nu_{21}$

**Fig. 8.** The ratio between effective elastic moduli and Poisson's ratio obtained using static Euler-Bernoulli beam theory and the corresponding classical expressions in Eqs. (89)–(93). The results are plotted as functions of $\alpha = t/l$ for a value of $\beta = h/l = 2$.

$$E_1 = \frac{4E\alpha^3}{\sqrt{3}(3\alpha^2+1)}, E_2 = \frac{4E\alpha^3}{\sqrt{3}(3\alpha^2+1)}, \nu_{12} = \frac{1-\alpha^2}{3\alpha^2+1}, \nu_{21} = \frac{1-\alpha^2}{3\alpha^2+1} \tag{109}$$

$$\text{and} \quad G_{12} = \frac{E\alpha^3}{\sqrt{3}(\alpha^2+1)} \tag{110}$$

It is useful to understand the contribution of the axial stretching on the values of the effective elastic moduli. In Fig. 8 we have shown the ratio of the expressions derived in this section to the corresponding classical expressions in Eqs. (89)–(93). This way it is possible to explicitly quantify the effect of axial stretching on the five quantities of interest. It is observed that values of $E_1$, $E_2$, $\nu_{12}$ and $\nu_{21}$ reduce upto 50% for certain values of θ compared with the classical expression when the thickness to length ratio α goes up to 0.25. It can also be observed that the cell angle θ also has a significant role on the reduced values when the axial stretching is taken into account. The shear modulus is relatively less impacted by the consideration of axial stretching. This is understandable due to the fact that the shear deformation is primarily bending dominated for the unit cell considered. A representative value of $\beta = h/l = 2$ is used in this figure.

### 4.2. Static elastic moduli with Timoshenko beam theory

The element stiffness matrix is obtained in Eq. (8) using the Timoshenko beam theory considers the shear deformation. When considering the static Timoshenko beam stiffness elements, the equivalent elastic properties are not functions of the frequency. Therefore, we omit the frequency dependence notation below. The necessary stiffness coefficients to obtain the expressions of $E_1$, $E_2$ $\nu_{12}$ and $\nu_{21}$ are

$$K_{55} = \frac{12}{1+\Phi}\frac{EI}{l^3} = \frac{Eb\alpha^3}{1+\Phi}, K_{44} = \frac{EA}{l} = Eb\alpha \quad \text{and} \quad K_{44}^{(h)} = \frac{EA}{h} = \frac{Eb\alpha}{\beta} \tag{111}$$

Using these, we obtain the ratios

$$\frac{K_{55}}{K_{44}} = \frac{\alpha^2}{1+\Phi} \quad \text{and} \quad \frac{K_{55}}{K_{44}^{(h)}} = \frac{\alpha^2\beta}{1+\Phi} \tag{112}$$

where from Eq. (9) we have

$$\Phi = \frac{2(1+\nu)}{k}\alpha^2 \tag{113}$$

Using the expressions of equivalent elastic moduli and Poisson's ratio from Eqs. ((54), (57), (64) and (67) we derive

$$E_1 = \frac{E\alpha^3\cos\theta}{(\beta+\sin\theta)\left((1+\Phi)\sin^2\theta+\alpha^2\cos^2\theta\right)} \tag{114}$$

$$E_2 = \frac{E\alpha^3(\beta+\sin\theta)}{(1+\Phi-\alpha^2)\cos^3\theta+\alpha^2(2\beta+1)\cos\theta} \tag{115}$$

$$\nu_{12} = \frac{\cos^2\theta(1+\Phi-\alpha^2)}{(\beta+\sin\theta)\sin\theta(1+\Phi+\alpha^2\cot^2\theta)} \tag{116}$$

$$\nu_{21} = \frac{(\beta+\sin\theta)\sin\theta(1+\Phi-\alpha^2)}{(1+\Phi-\alpha^2)\cos^2\theta+\alpha^2(2\beta+1)} \tag{117}$$

For the shear modulus, as before five elements from two different stiffness matrices are necessary. They are two coefficients of the $6\times6$ element stiffness matrix of the inclined member, namely, $K_{65}$, $K_{44}$ as in (111) with $K_{65} = -1/2\ \frac{Ebt^3}{l^2(1+\Phi)}$. For the element of the vertical member with half the length the shear correction factor can be obtained from Eq. (9) as

$$\Phi^{(h/2)} = \frac{2(1+\nu)}{k}\left(\frac{t}{h/2}\right)^2 = 4\,\frac{\Phi}{\beta^2} \tag{118}$$

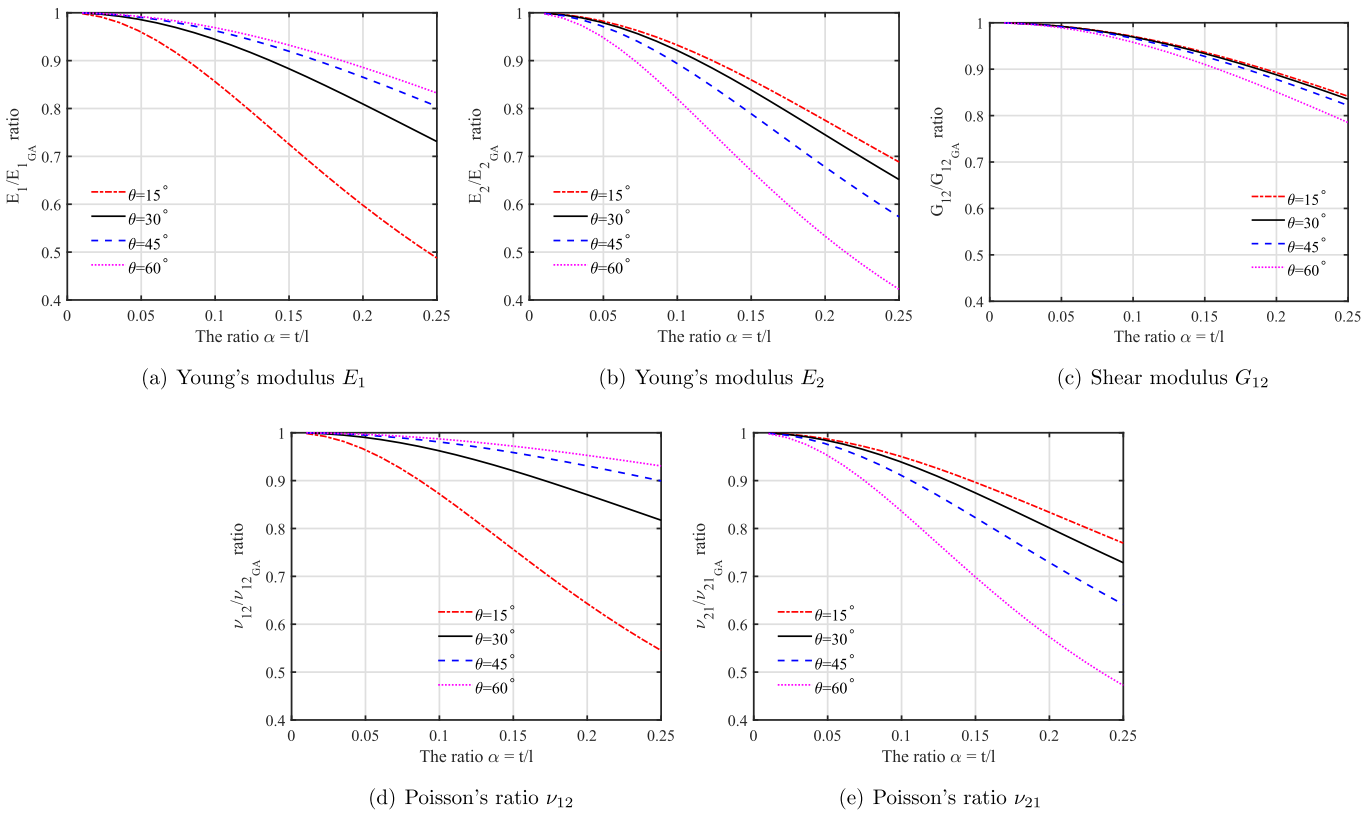


(a) Young's modulus $E_1$ (b) Young's modulus $E_2$ (c) Shear modulus $G_{12}$

(d) Poisson's ratio $\nu_{12}$ (e) Poisson's ratio $\nu_{21}$

**Fig. 9.** The ratio between effective elastic moduli and Poisson's ratio obtained using static Timoshenko beam theory and the corresponding classical expressions in Eqs. (89)–(93). The results are plotted as functions of $\alpha = t/l$ for a value of $\beta = h/l = 2$ and $\nu = 0.3$.

We also need three elements of the stiffness matrix of the vertical member with half the length given by

$$K_{55}^{(h/2)} = 8\,\frac{Ebt^3}{h^3}\left(1+4\,\frac{\Phi}{\beta^2}\right)^{-1}$$
$$K_{56}^{(h/2)} = -2\,\frac{Ebt^3}{h^2}\left(1+4\,\frac{\Phi}{\beta^2}\right)^{-1} \tag{119}$$

and

$$K_{66}^{(h/2)} = 2/3\,\frac{Ebt^3}{h}\left(1+4\,\frac{\Phi}{\beta^2}\right)^{-1}$$

Using these expressions, after some algebraic simplification, we obtain

$$G_{12} = \frac{E\alpha^3(\beta+\sin\theta)}{\left(\beta^2(1+\Phi+2\beta)+8\beta\Phi+\alpha^2(\cos\theta+(\beta+\sin\theta)\tan\theta)^2\right)\cos\theta} \tag{120}$$

Substituting $\Phi = 0$, the equations derived here reduce to the corresponding Euler-Bernoulli case discussed in the previous section.

For a regular lattice $\theta = \frac{\pi}{6}$ and $\beta = \frac{h}{l} = 1$. Substituting these in Eqs. (114)–(117) and (120) we have

$$E_1 = \frac{4E\alpha^3}{\sqrt{3}(3\alpha^2+1+\Phi)}, E_2 = \frac{4E\alpha^3}{\sqrt{3}(3\alpha^2+1+\Phi)}, \nu_{12} = \frac{1+\Phi-\alpha^2}{3\alpha^2+1+\Phi}$$
$$\nu_{21} = \frac{1+\Phi-\alpha^2}{3\alpha^2+1+\Phi}, \quad \text{and} \quad G_{12} = \frac{E\alpha^3}{\sqrt{3}(\alpha^2+1+3\Phi)} \tag{121}$$

If both the axial stretching and shear deformation are neglected, then substituting $\alpha^2 = 0$ and $\Phi = 0$ in the above expressions we have $E_1 = E_2 = (4/\sqrt{3})E\alpha^3 \approx 2.3E\alpha^3$, $\nu_{12} = \nu_{21} = 1$ and $G_{12} = (1/\sqrt{3})E\alpha^3 \approx 0.57E\alpha^3$. These match exactly with the values given in literature (Gibson and Ashby, 1999). In Fig. 9 we have shown the ratio of the expression derived in this section to the corresponding classical expressions in Eqs. (89)–(93). It is observed that values of $E_1$, $E_2$, $\nu_{12}$ and $\nu_{21}$ reduce up to 50% for certain values of θ compared to the classical expression when the thickness to length ratio α goes up to 0.25. To calculate the value of Φ in Eq. (113), we used the shape constant $k = 9/10$ and the Poisson's ratio of the underlying material as $\nu = 0.3$. It can be observed that the cell angle θ also has a significant role in the reduced values when the axial stretching is taken into account using the Timoshenko beam theory. The shear modulus is impacted more due to axial stretching compared to the case of the Euler-Bernoulli theory discussed in the previous section.

### 4.3. Elastic moduli with Euler-Bernoulli beam theory using dynamic finite element

Using the static Euler-Bernoulli beam theory, the element stiffness matrix is obtained in Eq. (6) and the element mass matrix is obtained in Eq. (15). The overall complex damped stiffness matrix is obtained from Eq. (18) by combining these matrices with the two damping factors. The frequency dependent complex stiffness coefficients are given by

$$K_{55}(\omega) = \frac{12EI}{l^3}(1+\mathrm{i}\omega c_k) + \left(-\omega^2+\mathrm{i}\omega c_m\right)\rho Al\frac{156}{420} = Eb\alpha^3\Gamma_1(\omega)$$
$$K_{44}(\omega) = \frac{EA}{l}(1+\mathrm{i}\omega c_k) + \left(-\omega^2+\mathrm{i}\omega c_m\right)\rho Al\frac{140}{420} = Eb\alpha\Gamma_2(\omega) \tag{122}$$

and

$$K_{44}^{(h)}(\omega) = \frac{EA}{h}(1+\mathrm{i}\omega c_k) + \left(-\omega^2+\mathrm{i}\omega c_m\right)\rho Ah\frac{140}{420} = \frac{Eb\alpha}{\beta}\Gamma_3(\omega)$$

In the above equations, the non-dimensional complex valued functions $\Gamma_j(\omega), j = 1, 2, 3$ can be simplified as

$$\Gamma_1(\omega) = (1+\mathrm{i}\omega c_k) - \frac{\omega^2}{\omega_0^2}\left(1-\mathrm{i}\frac{c_m}{\omega}\right)\frac{13}{420}$$
$$\Gamma_2(\omega) = (1+\mathrm{i}\omega c_k) - \frac{\omega^2}{\omega_0^2}\left(1-\mathrm{i}\frac{c_m}{\omega}\right)\frac{\alpha^2}{36} \quad (123)$$
$$\Gamma_3(\omega) = (1+\mathrm{i}\omega c_k) - \frac{\omega^2}{\omega_0^2}\left(1-\mathrm{i}\frac{c_m}{\omega}\right)\frac{\alpha^2\beta^2}{36}$$

where the frequency parameter corresponding to the bending vibration $\omega_0$ is given by

$$\omega_0 = \frac{1}{l^2}\sqrt{\frac{EI}{\rho A}} = \frac{\alpha}{2l}\sqrt{\frac{E}{3\rho}} \quad (124)$$

From the expressions in Eq. (122), we obtain the ratios

$$\frac{K_{55}(\omega)}{K_{44}(\omega)} = \alpha^2\frac{\Gamma_1(\omega)}{\Gamma_2(\omega)} \quad \text{and} \quad \frac{K_{55}(\omega)}{K_{44}^{(h)}(\omega)} = \alpha^2\beta\frac{\Gamma_1(\omega)}{\Gamma_3(\omega)} \quad (125)$$

Substituting the above expressions in Eqs. ((54), (57), (64) and (67) we have

$$E_1(\omega) = \frac{\Gamma_1(\omega)\Gamma_2(\omega)E\alpha^3\cos\theta}{(\beta+\sin\theta)\left(\Gamma_2(\omega)\sin^2\theta + \Gamma_1(\omega)\alpha^2\cos^2\theta\right)} \quad (126)$$

$$E_2(\omega) = \frac{\Gamma_1(\omega)\Gamma_2(\omega)\Gamma_3(\omega)E\alpha^3(\beta+\sin\theta)}{\Gamma_3(\omega)(\Gamma_2(\omega)-\Gamma_1(\omega)\alpha^2)\cos^3\theta + \Gamma_1(\omega)\alpha^2(2\beta\Gamma_2(\omega)+\Gamma_3(\omega))\cos\theta} \quad (127)$$

$$\nu_{12}(\omega) = \frac{\cos^2\theta(\Gamma_2(\omega)-\Gamma_1(\omega)\alpha^2)}{(\beta+\sin\theta)\sin\theta(\Gamma_2(\omega)+\Gamma_1(\omega)\alpha^2\cot^2\theta)} \quad (128)$$

$$\nu_{21}(\omega) = \frac{\Gamma_3(\omega)(\beta+\sin\theta)\sin\theta(\Gamma_2(\omega)-\Gamma_1(\omega)\alpha^2)}{\Gamma_3(\omega)(\Gamma_2(\omega)-\Gamma_1(\omega)\alpha^2)\cos^2\theta + \Gamma_1(\omega)\alpha^2(2\beta\Gamma_2(\omega)+\Gamma_3(\omega))} \quad (129)$$

For the shear modulus, five elements from two different stiffness matrices are necessary. They are two coefficients of the $6\times 6$ element stiffness matrix of the inclined member, namely $K_{44}$ as in (122) and

$$K_{65}(\omega) = -\frac{6EI}{l^2}(1+\mathrm{i}\omega c_k) - \left(-\omega^2+\mathrm{i}\omega c_m\right)\rho A l^2\frac{11}{210} = -\frac{Ebt^3}{2l^2}\Gamma_4(\omega) \quad (130)$$

where

$$\Gamma_4(\omega) = (1+\mathrm{i}\omega c_k) - \frac{\omega^2}{\omega_0^2}\left(1-\mathrm{i}\frac{c_m}{\omega}\right)\frac{11}{1260} \quad (131)$$

We additionally need three elements of the dynamic matrix of the vertical member with half the length

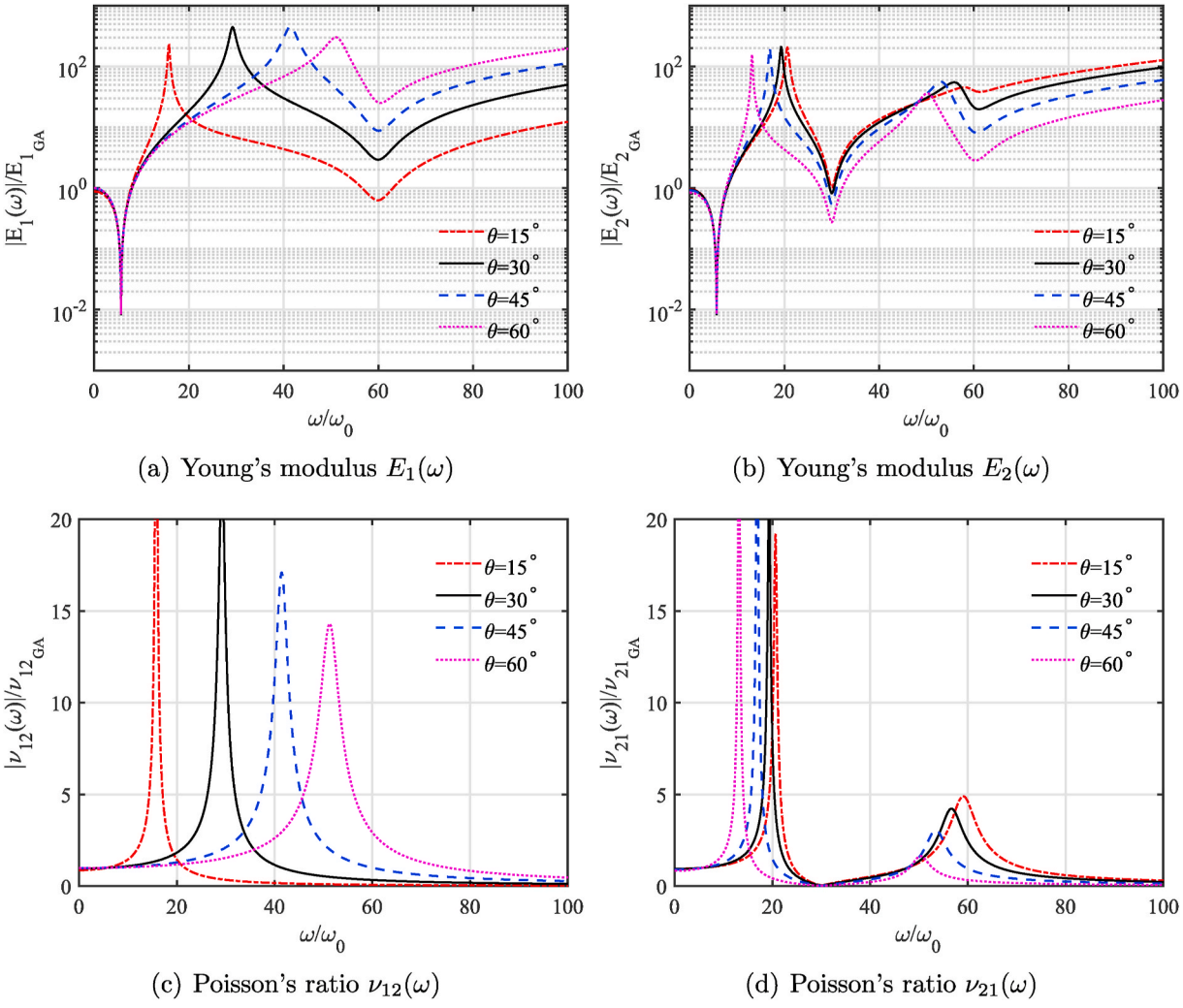


(a) Young's modulus $E_1(\omega)$ (b) Young's modulus $E_2(\omega)$

(c) Poisson's ratio $\nu_{12}(\omega)$ (d) Poisson's ratio $\nu_{21}(\omega)$

**Fig. 10.** The ratio between effective complex elastic moduli and Poisson's ratio obtained using Euler-Bernoulli beam theory and the corresponding classical expressions in Eqs. (89)–(93). The dynamic finite element approach is used and the absolute value of the results are plotted as functions of the normalised frequency $\omega/\omega_0$ for different values of the cell angle θ. The following values are used: $\alpha = t/l = 0.1$, $\beta = h/l = 2$ and the damping values $c_m = 10^{-2}$ and $c_k = 10^{-5}$.

$$K_{66}^{(h/2)}(\omega)=\frac{4EI}{(h/2)}(1+\mathrm{i}\omega c_k)+\left(-\omega^2+\mathrm{i}\omega c_m\right)\frac{\rho A(h/2)^3}{105}=\frac{2Ebt^3}{3h}\Gamma_5(\omega)$$
$$K_{56}^{(h/2)}(\omega)=-\frac{6EI}{(h/2)^2}(1+\mathrm{i}\omega c_k)-\left(-\omega^2+\mathrm{i}\omega c_m\right)\frac{11\rho A(h/2)^2}{210}=-\frac{2Ebt^3}{h^2}\Gamma_6(\omega)$$
$$K_{55}^{(h/2)}(\omega)=\frac{12EI}{(h/2)^3}(1+\mathrm{i}\omega c_k)+\left(-\omega^2+\mathrm{i}\omega c_m\right)\frac{13\rho A(h/2)}{35}=\frac{8Ebt^3}{h^3}\Gamma_7(\omega) \tag{132}$$

The non-dimensional functions $\Gamma_j(\omega), j=5,6,7$ are obtained as

$$\Gamma_5(\omega)=(1+\mathrm{i}\omega c_k)-\frac{\omega^2}{\omega_0^2}\left(1-\mathrm{i}\frac{c_m}{\omega}\right)\frac{\beta^4}{6720}$$
$$\Gamma_6(\omega)=(1+\mathrm{i}\omega c_k)-\frac{\omega^2}{\omega_0^2}\left(1-\mathrm{i}\frac{c_m}{\omega}\right)\frac{11\beta^4}{20160} \tag{133}$$
$$\Gamma_7(\omega)=(1+\mathrm{i}\omega c_k)-\frac{\omega^2}{\omega_0^2}\left(1-\mathrm{i}\frac{c_m}{\omega}\right)\frac{13\beta^4}{6720}$$

Substituting these expressions in the general equation for $G_{12}$ in Eq. (88) we obtain

$$G_{12}(\omega)=\frac{(\beta+\sin\theta)}{b\cos\theta}\frac{1}{\left(-\frac{h^2}{2lK_{65}(\omega)}+\frac{4K_{66}^{(h/2)}}{\left(K_{55}^{(h/2)}K_{66}^{(h/2)}-\left(K_{56}^{(h/2)}\right)^2\right)}+\frac{(\cos\theta+(\beta+\sin\theta)\tan\theta)^2}{K_{44}(\omega)}\right)}$$
$$=\frac{E\alpha^3(\beta+\sin\theta)\Gamma_2(\omega)\Gamma_4(\omega)\Gamma_8^2(\omega)}{\left(\beta^2\left(\Gamma_8^2(\omega)+2\Gamma_4(\omega)\Gamma_5(\omega)\beta\right)\Gamma_2(\omega)+\alpha^2(\cos\theta+(\beta+\sin\theta)\tan\theta)^2\Gamma_4(\omega)\Gamma_8^2(\omega)\right)\cos\theta} \tag{134}$$

where we define

$$\Gamma_8^2(\omega)=4\Gamma_5(\omega)\Gamma_7(\omega)-3\Gamma_6^2(\omega) \tag{135}$$

It can be easily deduced that in the zero frequency limit (that is, the static case)

$$\lim_{\omega\to 0}\Gamma_j(\omega)=1,\quad j=1,2,\cdots 8 \tag{136}$$

Using this limiting case, it can be verified that the frequency dependent expressions of the dynamic equivalent elastic moduli and Poisson's ratios derived here exactly reduce to the expressions derived in Subsection 4.1 for the respective static case. Substituting $\alpha^2=0$ along with the static limit, we can also verify that expressions in this section reduce to the corresponding classical expressions (89)–(93) as given in (Gibson and Ashby, 1999).

In Fig. 10 we have shown the ratio between the expression derived in this section and the corresponding classical expressions in Eqs. (89)–(93). This way it is possible to explicitly quantify the effect of axial stretching as a function of frequency. The damping values used here are $c_m=10^{-2}$ and $c_k=10^{-5}$ along with $\alpha=0.1$ and $\beta=2$. As the quantities in Eqs. (126)–(129) are complex-valued, their modulus are plotted in Fig. 10 for different cell angles. We only consider $E_1$, $E_2$, $\nu_{12}$ and $\nu_{21}$ and ignore $G_{12}$ as it is not significantly affected by axial stretching. It can be observed that $E_1$ and $E_2$ values can change by orders of magnitude depending on the frequency. We also observed that (results not shown here) the damping coefficients have a significant impact on the equivalent elastic properties of the lattice. Lower damping values results in sharper and higher peaks around the resonance-like frequency points. Results obtained using this approach are likely to be not very accurate at the higher frequency ranges due to the fact only one beam element is used in the unit cell model. The accuracy of these results will be verified by comparing to the exact dynamic stiffness method.

### 4.4. Elastic moduli with Timoshenko beam theory using dynamic finite element

The stiffness and the mass matrix of a beam element using the Timoshenko beam theory are given by Eqs. (8) and (16). Combining the approaches presented in the previous two sections, it is possible to obtain the frequency dependent expressions of the dynamic equivalent elastic moduli and Poisson's ratios in closed-form. Using the expressions of equivalent elastic moduli and Poisson's ratio from Eqs. ((54), (57), (64) and (67), after some algebraic simplifications, we obtain

$$E_1(\omega)=\frac{\Gamma_1(\omega)\Gamma_2(\omega)E\alpha^3\cos\theta}{(\beta+\sin\theta)\left((1+\Phi)\Gamma_2(\omega)\sin^2\theta+\Gamma_1(\omega)\alpha^2\cos^2\theta\right)} \tag{137}$$

$$E_2(\omega)=\frac{\Gamma_1(\omega)\Gamma_2(\omega)\Gamma_3(\omega)E\alpha^3(\beta+\sin\theta)}{\Gamma_3(\omega)((1+\Phi)\Gamma_2(\omega)-\Gamma_1(\omega)\alpha^2)\cos^3\theta+\Gamma_1(\omega)\alpha^2(2\beta\Gamma_2(\omega)+\Gamma_3(\omega))\cos\theta} \tag{138}$$

$$\nu_{12}(\omega)=\frac{\cos^2\theta((1+\Phi)\Gamma_2(\omega)-\Gamma_1(\omega)\alpha^2)}{(\beta+\sin\theta)\sin\theta((1+\Phi)\Gamma_2(\omega)+\Gamma_1(\omega)\alpha^2\cot^2\theta)} \tag{139}$$

$$\nu_{21}(\omega)=\frac{\Gamma_3(\omega)(\beta+\sin\theta)\sin\theta((1+\Phi)\Gamma_2(\omega)-\Gamma_1(\omega)\alpha^2)}{\Gamma_3(\omega)((1+\Phi)\Gamma_2(\omega)-\Gamma_1(\omega)\alpha^2)\cos^2\theta+\Gamma_1(\omega)\alpha^2(2\beta\Gamma_2(\omega)+\Gamma_3(\omega))} \tag{140}$$

$$G_{12}(\omega)=\frac{E\alpha^3(\beta+\sin\theta)\Gamma_2(\omega)\Gamma_4(\omega)\Gamma_8^2(\omega)}{\beta^2((1+\Phi)\Gamma_8^2(\omega)+2\Gamma_4(\omega)\Gamma_5(\omega)\beta)\Gamma_2(\omega)+8\beta\Phi\Gamma_2(\omega)\Gamma_4(\omega)\Gamma_5(\omega)+\alpha^2(\cos\theta+(\beta+\sin\theta)\tan\theta)^2\Gamma_4\left(\omega\right)\Gamma_8^2\left(\omega\right)\Big)} \tag{141}$$

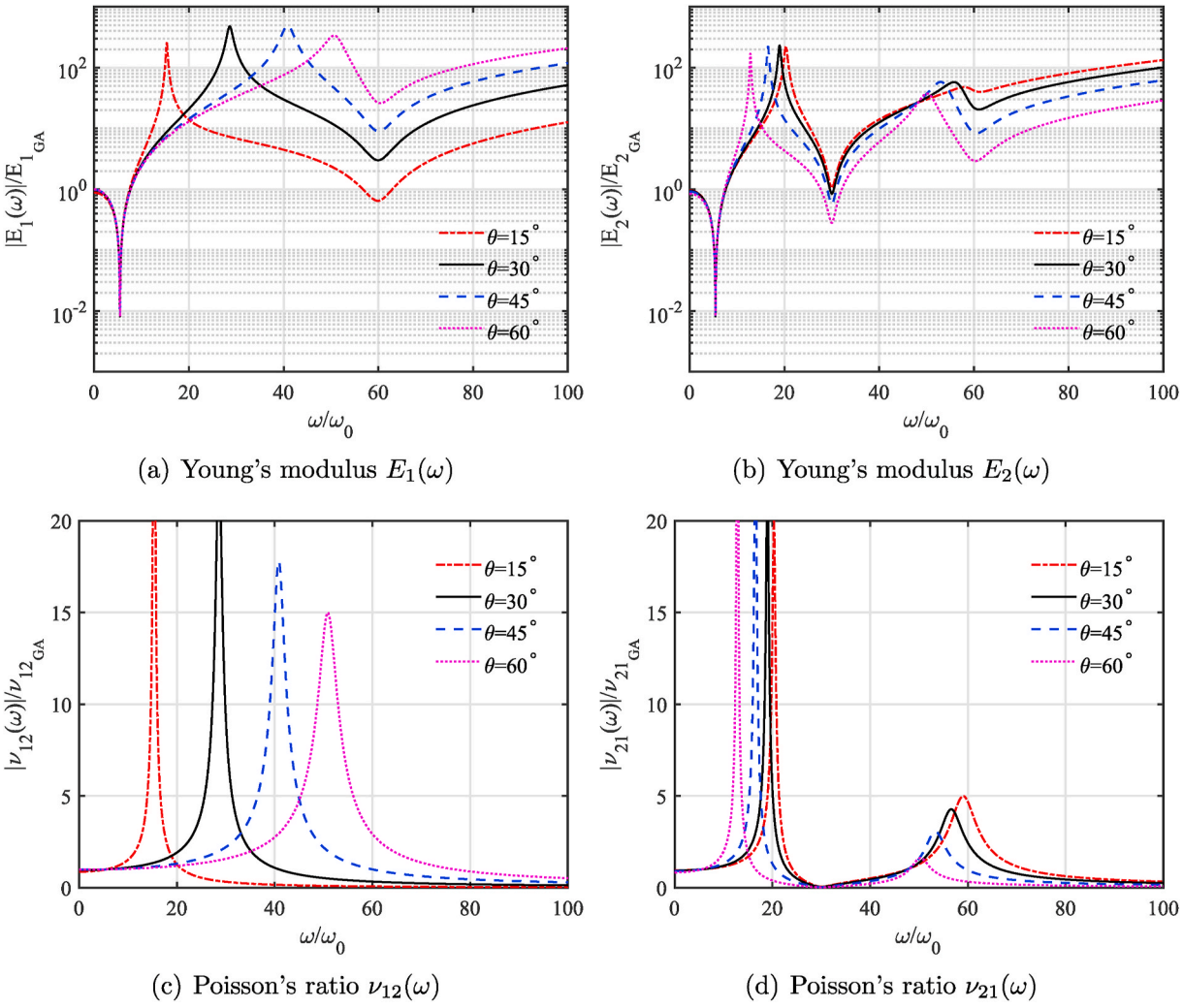


**Fig. 11.** The ratio between effective complex elastic moduli and Poisson's ratio obtained using Timoshenko beam theory and the corresponding classical expressions in Eqs. (89)–(93). The dynamic finite element approach is used and the absolute value of the results are plotted as functions of the normalised frequency $\omega/\ \omega_0$ for different values of the cell angle θ. The following values are used: $\alpha = t/l = 0.1$, $\beta = h/l = 2$ and the damping values $c_m = 10^{-2}$ and $c_k = 10^{-5}$.

The non-dimensional complex valued frequency-dependent functions $\Gamma_j(\omega), j = 1, 2, \cdots 8$ are derived in closed-form as

$$\begin{aligned}
\Gamma_1(\omega) &= (1+\mathrm{i}\omega c_k) - \frac{\omega^2}{\omega_0^2}\left(1-\mathrm{i}\frac{c_m}{\omega}\right)\left(\frac{13}{420}+\frac{7}{120}\Phi+\frac{1}{36}\Phi^2\right)\\
\Gamma_2(\omega) &= (1+\mathrm{i}\omega c_k) - \frac{\omega^2}{\omega_0^2}\left(1-\mathrm{i}\frac{c_m}{\omega}\right)\frac{\alpha^2}{36}\\
\Gamma_3(\omega) &= (1+\mathrm{i}\omega c_k) - \frac{\omega^2}{\omega_0^2}\left(1-\mathrm{i}\frac{c_m}{\omega}\right)\frac{\alpha^2\beta^2}{36}\\
\Gamma_4(\omega) &= (1+\mathrm{i}\omega c_k) - \frac{\omega^2}{\omega_0^2}\left(1-\mathrm{i}\frac{c_m}{\omega}\right)\left(\frac{11}{1260}+\frac{11}{720}\Phi+\frac{1}{144}\Phi^2\right)\\
\Gamma_5(\omega) &= (1+\mathrm{i}\omega c_k) - \frac{\omega^2}{\omega_0^2}\left(1-\mathrm{i}\frac{c_m}{\omega}\right)\frac{\beta^4}{6720}\left(1+\frac{7}{4}\Phi+\frac{7}{8}\Phi^2\right)\\
\Gamma_6(\omega) &= (1+\mathrm{i}\omega c_k) - \frac{\omega^2}{\omega_0^2}\left(1-\mathrm{i}\frac{c_m}{\omega}\right)\frac{\beta^4}{20160}\left(11+\frac{77}{4}\Phi+\frac{35}{4}\Phi^2\right)\\
\Gamma_7(\omega) &= (1+\mathrm{i}\omega c_k) - \frac{\omega^2}{\omega_0^2}\left(1-\mathrm{i}\frac{c_m}{\omega}\right)\frac{\beta^4}{6720}\left(13+\frac{49}{2}\Phi+\frac{35}{3}\Phi^2\right)\\
\Gamma_8^2(\omega) &= 4\Gamma_5(\omega)\Gamma_7(\omega) - 3\Gamma_6^2(\omega)
\end{aligned} \tag{142}$$

Comparing equivalent expressions for $\Gamma_j(\omega)$ for the Euler-Bernoulli case given by Eqs. (123), (131) and (133), one can deduce that these are a special case of Eq. (142) when $\Phi = 0$. Therefore, the closed-from expressions derived here explicitly quantifies the contribution of the shear correction factor $\Phi$ on the Euler-Bernoulli based expressions derived in the previous subsection. It can be easily deduced that in the zero-frequency limit all $\Gamma_j(\omega), j = 1, 2, \cdots 8$ approach to unity. Using this limiting case, it can be verified that the frequency-dependent expressions of the dynamic equivalent elastic moduli and Poisson's ratios derived here exactly reduce to the expressions derived in Subsection 4.2 for the respective static case.

In Fig. 11 we have shown the ratio between the expression derived in this section and the corresponding classical expressions in Eqs. (89)–(93). This way it is possible to explicitly quantify the effect of axial stretching as a function of frequency. The damping values used here are $c_m = 10^{-2}$ and $c_k = 10^{-5}$ along with $\alpha = 0.1$ and $\beta = 2$. To calculate the value of $\Phi$ in Eq. (113), we used the shape constant $k = 9/10$ and the Poisson's ratio of the underlying material as $\nu = 0.3$. As the quantities in Eqs. (137)–(140) are complex-valued, their modulus are plotted in Fig. 11 for different cell angles. It can be observed that $E_1$ and $E_2$ values can change by orders of magnitude depending on the frequency. The results obtained here are qualitatively similar to what obtained in the previous subsection using the Euler-Bernoulli beam theory, though they vary quantitatively. In the following subsections, we use dynamic stiffness matrix to discuss the accuracy of dynamic elastic moduli obtained using dynamic finite element method.

### 4.5. Elastic moduli with Euler-Bernoulli beam theory using dynamic stiffness

In subsubsection 2.5.2, the dynamic stiffness matrix using Euler-Bernoulli beam theory was derived. Combining this with the dynamic stiffness matrix due to the axial motion, the complete $6\times 6$ matrix is given by Eq. (49). From the derivations in Subsection 3.1 and Subsection 3.2, it can be observed that two coefficients of the $6\times 6$ dynamic stiffness matrix of the inclined member and one coefficients of the $6\times 6$ dynamic stiffness matrix of the vertical member, namely, $K_{55}(\omega)$, $K_{44}(\omega)$ and $K_{44}^{(h)}(\omega)$, are necessary to obtain $E_1$, $E_2$ $\nu_{12}$ and $\nu_{21}$. Using the expressions of moment of inertia and the cross-sectional area in Eqs. (11) and (12), the stiffness coefficients are given by

$$\begin{aligned}
K_{55}(\omega) &= \frac{\overline{E}Ik_b^3}{l^3}(cS+sC)/\delta = \overline{E}b\alpha^3\underbrace{\frac{1}{12}k_b^3(cS+sC)/\delta}_{\Gamma_1(\omega)}\\
K_{44}(\omega) &= a_1 = \frac{\overline{E}A}{l}k_a\cot(k_a) = \overline{E}b\alpha\underbrace{k_a\cot(k_a)}_{\Gamma_2(\omega)}\\
K_{44}^{(h)}(\omega) &= \frac{\overline{E}A}{h}k_a^{(h)}\cot\left(k_a^{(h)}\right) = \frac{\overline{E}b\alpha}{\beta}k_a^{(h)}\cot\left(k_a^{(h)}\right) = \frac{\overline{E}b\alpha}{\beta}\underbrace{\beta k_a\cot\beta k_a}_{\Gamma_3(\omega)}
\end{aligned} \tag{143}$$

From the derivations in subsection 2.5.1 and subsection 2.5.2, in the above equations we have

$$\begin{aligned}
\overline{E} &= E(1+\mathrm{i}\omega c_k)\\
k_b^4 &= \frac{\rho A\omega^2L^4(1-\mathrm{i}c_m/\omega)}{\overline{E}I} = \frac{\omega^2}{\omega_0^2}\frac{(1-\mathrm{i}c_m/\omega)}{(1+\mathrm{i}\omega c_k)}\\
k_a^2 &= \frac{\alpha^2}{12}k_b^4 \quad \text{and} \quad k_a^{(h)^2} = \beta^2k_a^2
\end{aligned} \tag{144}$$

As the expressions in Eq. (143) have the same mathematical form as the expressions in Eq. (122), the equivalent elastic moduli and Poisson's ratios are given by exactly the same expressions in Eqs. 126–129 noting the difference in the definitions of the complex frequency dependent functions $\Gamma_j(\omega), j = 1, 2, 3$. Upon some algebraic simplifications, we obtain the closed-form expressions

$$E_1(\omega) = \frac{\overline{E}\alpha^3k_b^3(sC+cS)\cos\theta}{(\beta+\sin\theta)\left(12\delta\sin^2\theta+\alpha^2\cos^2\theta\frac{k_b^3(sC+cS)}{k_a\cot k_a}\right)} \tag{145}$$

$$E_2(\omega) = \frac{\overline{E}\alpha^3k_b^3(sC+cS)(\beta+\sin\theta)}{12\delta\cos^3\theta+\alpha^2\left(\sin^2\theta+2\cot k_a/\cot\beta k_a\right)\cos\theta\frac{k_b^3(sC+cS)}{k_a\cot k_a}} \tag{146}$$

$$\nu_{12}(\omega) = \frac{\cos^2\theta\left(12\delta k_a\cot k_a-\alpha^2k_b^3(sC+cS)\right)}{(\beta+\sin\theta)\sin\theta\left(12\delta k_a\cot k_a+\alpha^2k_b^3(sC+cS)\cot^2\theta\right)} \tag{147}$$

$$\nu_{21}(\omega) = \frac{(\beta+\sin\theta)\sin\theta\left(12\delta k_a\cot k_a-\alpha^2k_b^3(sC+cS)\right)}{12\delta\cos^2\theta+\alpha^2\left(\sin^2\theta+2\cot k_a/\cot\beta k_a\right)\frac{k_b^3(sC+cS)}{k_a\cot k_a}} \tag{148}$$

Here the frequency-dependent complex quantities are given by

$$\begin{aligned}
&\delta = 1-cC\\
&\text{and} \quad s=\sin k_b, \quad c=\cos k_b, \quad S=\sinh k_b, \quad C=\cosh k_b
\end{aligned} \tag{149}$$

For the shear modulus, five elements from two different stiffness matrices are necessary. They are two coefficients of the $6\times 6$ element stiffness matrix of the inclined member, namely $K_{44}$ as in Eq. (143) and three coefficients of the vertical member of length $h/2$. The frequency parameter of this element can be expressed as

$$k_b^{(h/2)} = \beta k_b/2 \tag{150}$$

where $k_b$ is given in Eq. (144). Using this, the necessary dynamic stiffness coefficients can be obtained as

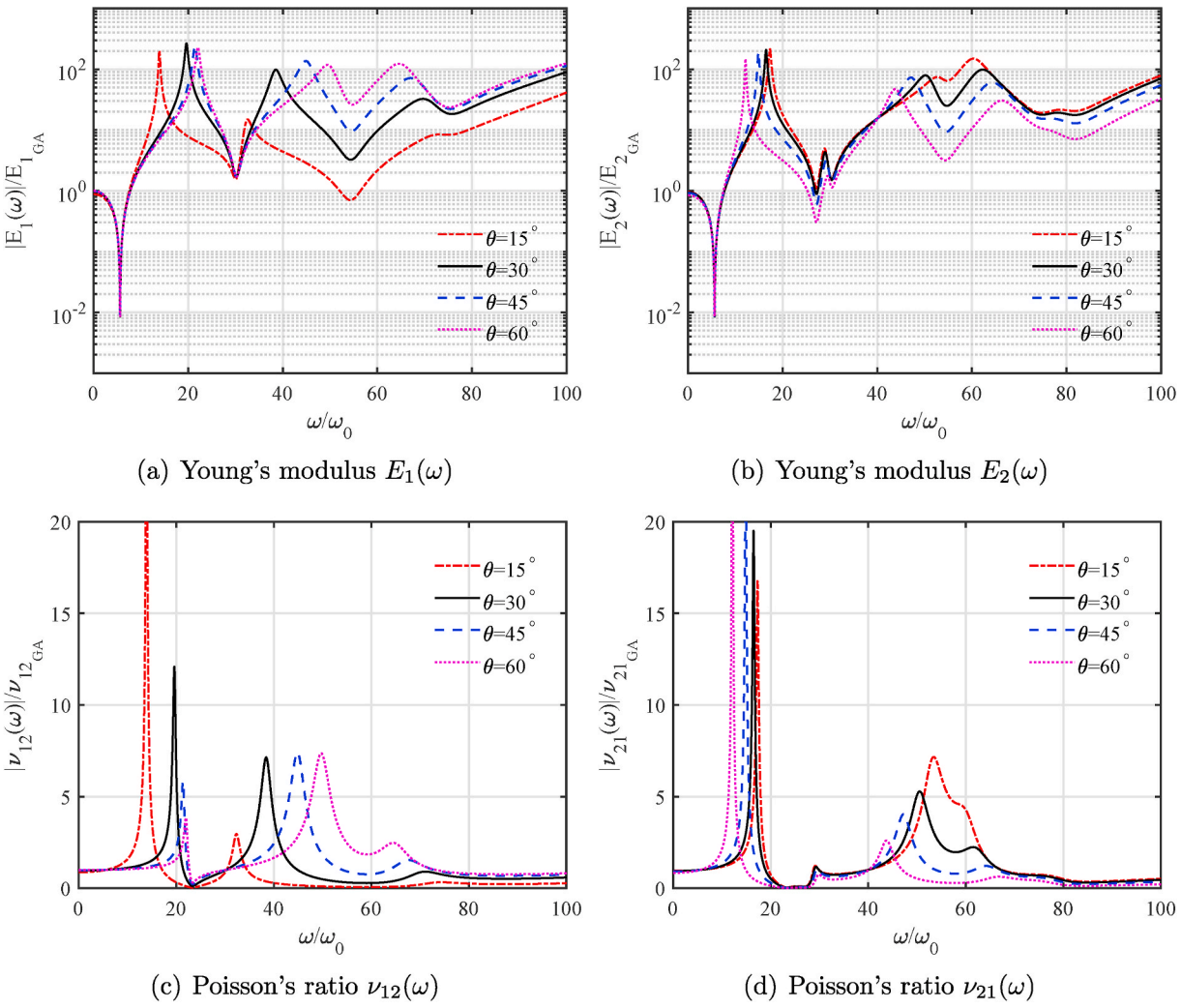


**Fig. 12.** The ratio between, effective complex elastic moduli and Poisson's ratio obtained using dynamic stiffness method with the Euler-Bernoulli beam theory, and the corresponding classical expressions in Eqs. (89)–(93). Absolute value of the results are plotted as functions of the normalised frequency $\omega/\ \omega_0$ for different cell angles θ. The following values are used: $\alpha = t/l = 0.1$, $\beta = h/l = 2$ and the damping constants are $c_m = 10^{-2}$ and $c_k = 10^{-5}$.

$$
\begin{aligned}
K_{65}(\omega) &= -6\frac{\overline{E}I}{l^2}\left(1/6\ \frac{k_b^2 sS}{\delta}\right) = -\frac{Ebt^3}{2l^2}\underbrace{\frac{k_b^2 sS}{6\delta}}_{\Gamma_4(\omega)}\\
K_{66}^{(h/2)}(\omega) &= \frac{4\overline{E}I}{(h/2)}\left(1/8\ \frac{k_b\beta\,(C_\beta s_\beta - S_\beta c_\beta)}{\delta_\beta}\right) = \frac{2\overline{E}bt^3}{3h}\underbrace{\frac{k_b\beta\,(C_\beta s_\beta - S_\beta c_\beta)}{8\delta_\beta}}_{\Gamma_5(\omega)}\\
K_{56}^{(h/2)}(\omega) &= -\frac{6\overline{E}I}{(h/2)^2}\left(1/24\ \frac{k_b^2\beta^2 s_\beta S_\beta}{\delta_\beta}\right) = -\frac{2\overline{E}bt^3}{h^2}\underbrace{\frac{k_b^2\beta^2 s_\beta S_\beta}{24\delta_\beta}}_{\Gamma_6(\omega)}\\
K_{55}^{(h/2)}(\omega) &= \frac{12\overline{E}I}{(h/2)^3}\left(\frac{k_b^3\beta^3(C_\beta s_\beta + S_\beta c_\beta)}{96\ \delta_\beta}\right) = \frac{8\overline{E}bt^3}{h^3}\underbrace{\frac{k_b^3\beta^3(C_\beta s_\beta + S_\beta c_\beta)}{96\ \delta_\beta}}_{\Gamma_7(\omega)}
\end{aligned}
\tag{151}
$$

Here

$$
\begin{aligned}
&\delta_\beta = 1 - c_\beta C_\beta,\\
&s_\beta = \sin(\beta k_b/2),\quad c_\beta = \cos(\beta k_b/2),\quad S_\beta = \sinh(\beta k_b/2),\quad C_\beta = \cosh(\beta k_b/2)
\end{aligned}
\tag{152}
$$

As the expressions in (151) have the same mathematical form as the expressions in (130) and (132), the equivalent shear modulus can be obtained using Eq. (134) noting the difference in the definitions of the complex frequency dependent functions $\Gamma_j(\omega), j = 4, \cdots 7$. Upon some algebraic simplifications, we obtain the closed-form expressions

$$
G_{12}(\omega) = \frac{\overline{E}\alpha^3 k_b^3 k_a \cos k_a G_1(\beta + \sin\theta)}{\left(6\delta k_a \cos k_a G_2 + \alpha^2 \sin k_a G_1 k_b^3(\cos\theta + (\beta + \sin\theta)\tan\theta)^2\right)\cos\theta}
\tag{153}
$$

with

$$
\begin{aligned}
&G_1 = Ss\left(\left(s_\beta^2 + 1\right)S_\beta^2 - s_\beta^2\right)\\
&\text{and}\\
&G_2 = \delta\, k_b(C_\beta s_\beta - S_\beta)(C_\beta s_\beta + S_\beta)\beta^2 + 8\, Ss\delta_\beta(C_\beta s_\beta - S_\beta c_\beta)
\end{aligned}
\tag{154}
$$

It can be proved that in the zero-frequency limit all $\Gamma_j(\omega), j = 1, 2, \cdots 7$ approach to unity. Using this limiting case, it can be verified that the

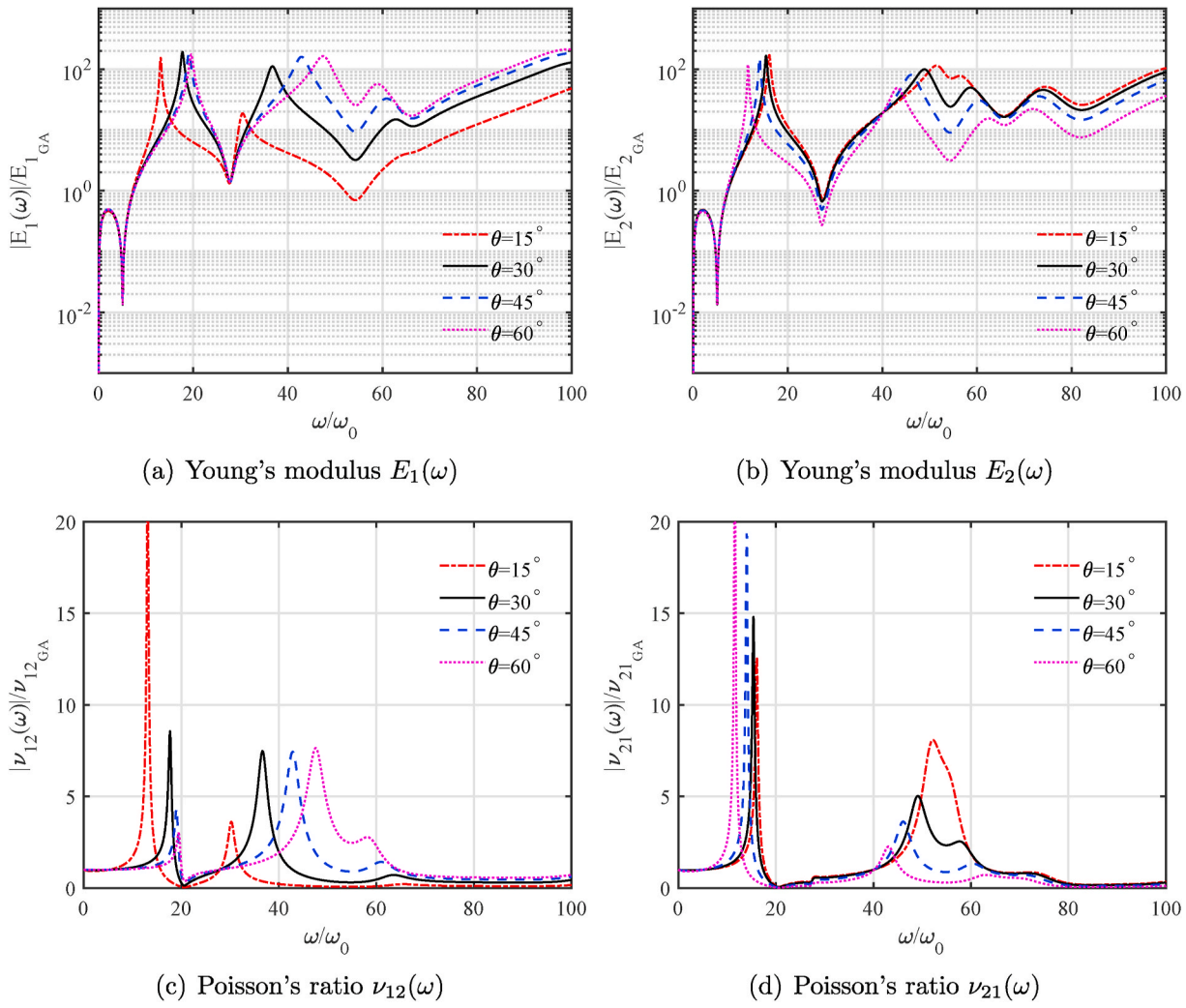


**Fig. 13.** The ratio between, effective complex elastic moduli and Poisson's ratio obtained using dynamic stiffness method with the Timoshenko beam theory, and the corresponding classical expressions in Eqs. (89)–(93). Absolute value of the results are plotted as functions of the normalised frequency $\omega/\omega_0$ for different cell angles θ. The following values are used: $\alpha = t/l = 0.1$, $\beta = h/l = 2$ and the damping constants are $c_m = 10^{-2}$ and $c_k = 10^{-5}$.

frequency-dependent expressions of the dynamic equivalent elastic moduli and Poisson's ratios derived here exactly reduce to the expressions derived in Subsection 4.1 for the respective static case. If the axial stretching is neglected ($\alpha^2 \to 0$), then the expressions derived here reduce to what obtained in reference (Mukhopadhyay et al., 2019b). Such analytical exact form of validations using the special cases provide adequate confidence on the developed formulae.

In Fig. 12 we have shown the ratio between the expressions derived in this section and the corresponding classical expressions in Eqs. (89)–(93). The damping values used here are $c_m = 10^{-2}$ and $c_k = 10^{-5}$ along with $\alpha = 0.1$ and $\beta = 2$. As the quantities in Eq. (126)–(129) are complex-valued, their modulus are plotted in Fig. 12 for different cell angles. It can be observed that $E_1$ and $E_2$ values can change by orders of magnitude depending on the frequency. The results obtained using this approach are accurate as the dynamic stiffness method is exact for any frequency ranges. Compared to the equivalent results in Fig. 10, it can be observed that more details of the dynamic behaviour at the higher frequency ranges have been captured here. This, in turn, provides the significance of adopting dynamic stiffness approach instead of a dynamic finite element approach with a single beam element as the members of the unit cells. A higher degree of discretization in the dynamic finite element approach would improve the result, but at the cost of more computational intensiveness and inability to have presentable closed-form expressions.

### 4.6. Elastic moduli with Timoshenko beam theory using dynamic stiffness

Following a procedure similar to the previous section, the necessary stiffness coefficients are obtained as

$$K_{55}(\omega) = \frac{\overline{E}I\overline{b}^2}{l^3}\frac{(\lambda_2+\eta\lambda_1)(cS+\eta sC)}{(\lambda_1\lambda_2\delta)} = \overline{E}b\alpha^3\underbrace{\frac{1}{12}\overline{b}^2\frac{(\lambda_2+\eta\lambda_1)(cS+\eta sC)}{(\lambda_1\lambda_2\delta)}}_{\Gamma_1(\omega)}$$

$$K_{44}(\omega) = a_1 = \frac{\overline{E}A}{l}k_a\cot(k_a) = \overline{E}b\alpha\underbrace{k_a\cot(k_a)}_{\Gamma_2(\omega)}$$

$$K_{44}^{(h)}(\omega) = \frac{\overline{E}A}{h}k_a^{(h)}\cot\left(k_a^{(h)}\right) = \frac{\overline{E}b\alpha}{\beta}k_a^{(h)}\cot\left(k_a^{(h)}\right) = \frac{\overline{E}b\alpha}{\beta}\underbrace{\beta k_a\cot\beta k_a}_{\Gamma_3(\omega)} \tag{155}$$

From the derivations in subsubsection 2.5.1 and subsubsection 2.5.2, in the above equations we have

$$\overline{b}^2 = \frac{\rho A\omega^2L^4(1-\mathrm{i}c_m/\omega)}{EI(1+\mathrm{i}\omega c_k)} = \frac{\omega^2}{\omega_0^2}\frac{(1-\mathrm{i}c_m/\omega)}{(1+\mathrm{i}\omega c_k)}$$
$$k_a^2 = \frac{\alpha^2}{12}\overline{b}^2 \quad \text{and} \quad k_a^{(h)^2} = \beta^2k_a^2 \tag{156}$$

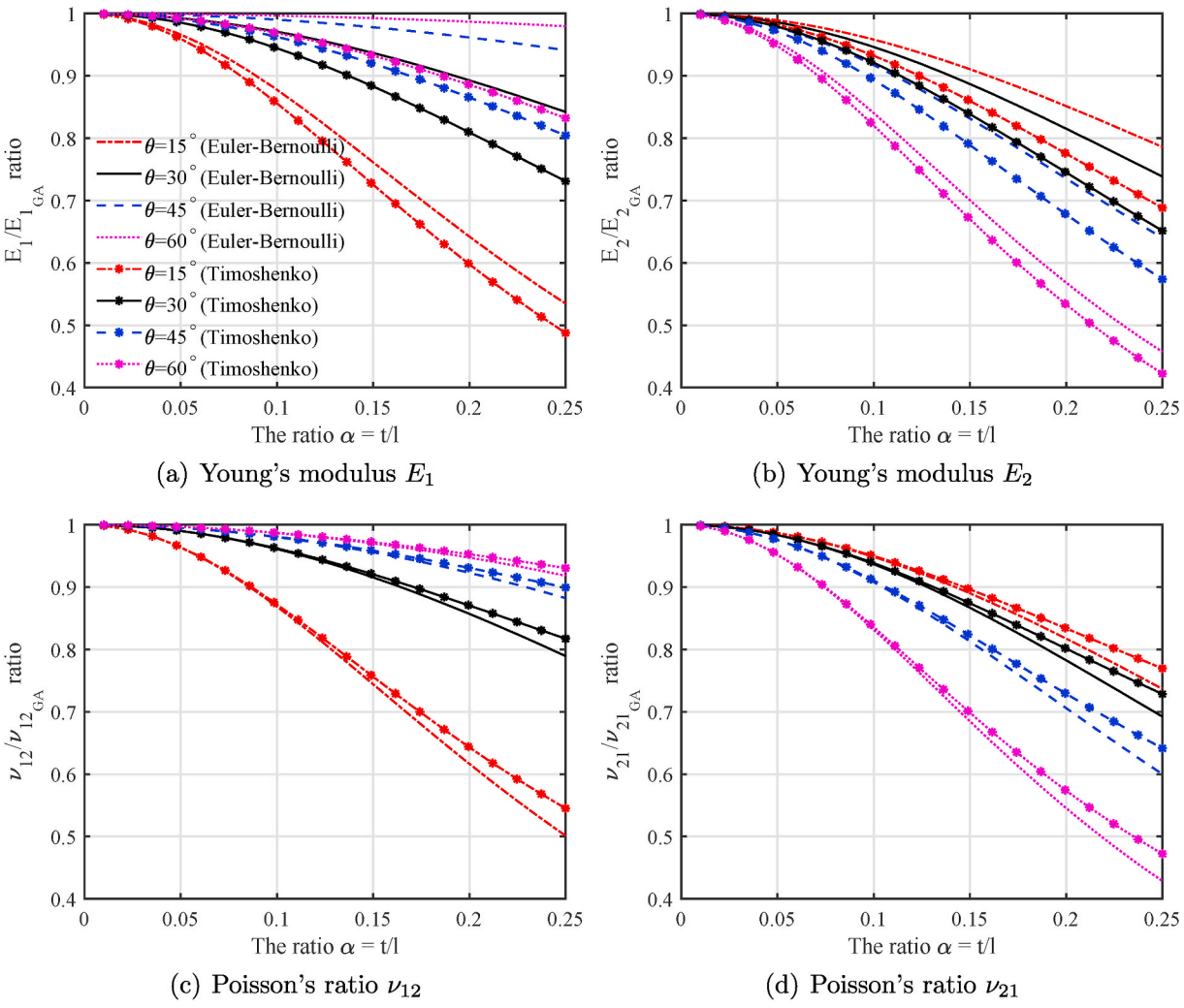


**Fig. 14.** The comparison of normalised effective elastic moduli and Poisson's ratio obtained using two static approaches. The results are plotted as functions of $\alpha = t/l$ for a value of $\beta = h/l = 2$ and $\nu = 0.3$ and different cell angles θ.

As the expressions in Eq. (155) have the same mathematical form as the expressions in Eq. (122), the equivalent elastic moduli and Poisson's ratios are given by exactly the same expressions in Eqs. 126–129 noting the difference in the definitions of the complex frequency dependent functions $\Gamma_j(\omega), j = 1, 2, 3$. Upon some algebraic simplifications, we obtain the closed-form expressions

$$E_1(\omega) = \frac{\overline{E}\alpha^3\overline{b}^2(\lambda_2+\eta\lambda_1)(\eta sC+cS)\cos\theta}{(\beta+\sin\theta)\left(12\delta\lambda_1\lambda_2\sin^2\theta+\alpha^2\cos^2\theta\left(\frac{\overline{b}^2(\lambda_2+\eta\lambda_1)(\eta sC+cS)}{k_a\cot k_a}\right)\right)} \tag{157}$$

$$E_2(\omega) = \frac{\overline{E}\alpha^3\overline{b}^2(\lambda_2+\eta\lambda_1)(\eta sC+cS)(\beta+\sin\theta)}{12\delta\lambda_1\lambda_2\cos^3\theta+\alpha^2\left(\sin^2\theta+2\cot k_a/\cot\beta k_a\right)\cos\theta\left(\frac{\overline{b}^2(\lambda_2+\eta\lambda_1)(\eta sC+cS)}{k_a\cot k_a}\right)} \tag{158}$$

$$\nu_{12}(\omega) = \frac{\cos^2\theta\left(2\delta\lambda_1\lambda_2k_a\cot k_a-\alpha^2\overline{b}^2(\lambda_2+\eta\lambda_1)(\eta sC+cS)\right)}{(\beta+\sin\theta)\sin\theta\left(12\delta k_a\cot k_a+\alpha^2\overline{b}^2(\lambda_2+\eta\lambda_1)(\eta sC+cS)\cot^2\theta\right)} \tag{159}$$

$$\nu_{21}(\omega) = \frac{(\beta+\sin\theta)\sin\theta\left(2\delta\lambda_1\lambda_2k_a\cot k_a-\alpha^2\overline{b}^2(\lambda_2+\eta\lambda_1)(\eta sC+cS)\right)}{12\delta\lambda_1\lambda_2\cos^2\theta+\alpha^2\left(\sin^2\theta+2\cot k_a/\cot\beta k_a\right)\left(\frac{\overline{b}^2(\lambda_2+\eta\lambda_1)(\eta sC+cS)}{k_a\cot k_a}\right)} \tag{160}$$

The shear modulus can also be obtained following a procedure similar to the previous section. However, the resulting closed-form expression is not simple and presentable and is omitted here. It is suggested to use the general formula for $G_{12}$ in Eq. (88) together with the elements of the dynamic stiffness matrix derived in subsubsection 2.5.3.

In Fig. 13 we have shown the ratio between the expression derived in this section and the corresponding classical expressions in Eqs. (89)–(93). The damping values used here are $c_m = 10^{-2}$ and $c_k = 10^{-5}$ along with $\alpha = 0.1$ and $\beta = 2$. As the quantities in Eq. (137)–(140) are complex valued, their modulus are plotted in Fig. 13 for different cell angles. It can be observed that $E_1$ and $E_2$ values can change by orders of magnitude depending on the frequency. The results obtained using this approach are accurate as the dynamic stiffness method is exact for any frequency ranges. Compared to the equivalent results in Fig. 11, it can be observed that more details of the dynamic behaviour at the higher frequency ranges have been captured here.

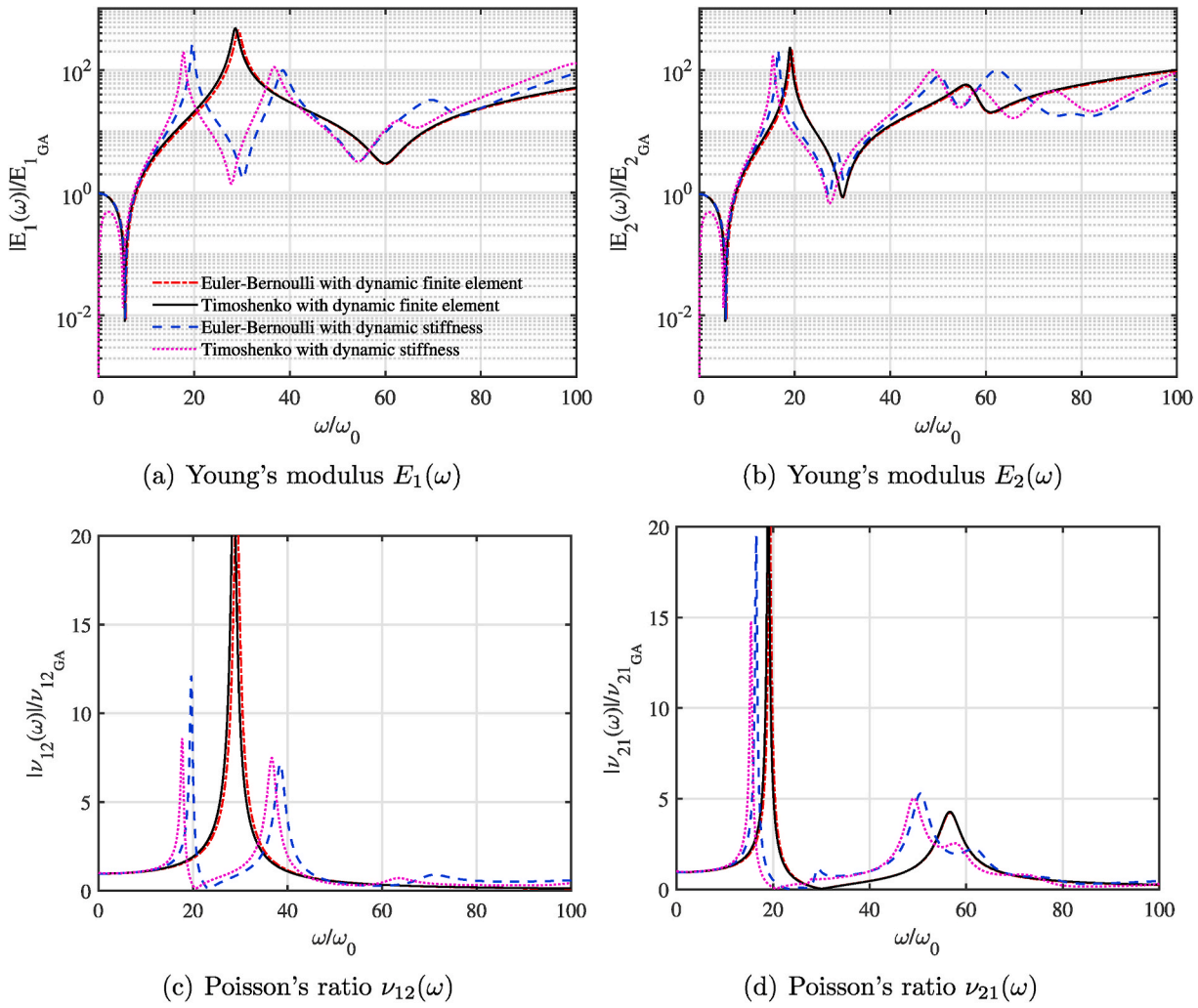


**Fig. 15.** The comparison of normalised effective complex elastic moduli and Poisson's ratio obtained using four dynamic approaches. Absolute value of the results are compared as functions of the normalised frequency $\omega/\omega_0$ for a cell angle of $\theta = 30^\circ$. The following values are used: $\alpha = t/l = 0.1$, $\beta = h/l = 2$ and the damping constants are $c_m = 10^{-2}$ and $c_k = 10^{-5}$.

### *4.7. Discussions on the results*

In the previous subsections, effective elastic moduli and Poisson's ratio of the lattice were obtained using six different approaches. Here we aim to compare and contrast the results presented and develop physical interpretations. In Fig. 14, two Young's moduli and Poisson's ratio obtained using the Euler-Bernoulli and Timoshenko beam approaches have been compared. The analytical derivations corresponding to the two approaches are given in Subsection 4.1 and Subsection 4.2. The values of both Young's moduli become lower when using the Timoshenko beam theory compared to the Euler-Bernoulli beam theory. This is expected as the Timoshenko beam theory incudes the deformation due to shear and therefore it is mechanically a less rigid model. For higher $t/\,l$ ratios, the differences can be significant for certain values of the cell angle $\theta$. Compared to the elastic moduli, the differences between the Poisson's ratios obtained using the Euler-Bernoulli and Timoshenko beam are less. Recall that the values plotted in Fig. 14 are normalised with respect to the classical results (Gibson and Ashby, 1999) given in Eq. (89) – (92). Therefore, when the axial deformations are included, regardless of what beam theory is used, the values of the effective elastic moduli and Poisson's ratio of the lattice are reduced.

In Fig. 15, results obtained from four dynamic approaches are compared. We consider the normalised values of $E_1(\omega), E_2(\omega), \nu_{12}(\omega)$ and $\nu_{21}(\omega)$. The four methods compared here are Euler-Bernoulli beam theory with the dynamic finite element (Subsection 4.3), Timoshenko beam theory with the dynamic finite element (Subsection 4.4), Euler-Bernoulli beam theory with the dynamic stiffness approach (Subsection 4.5) and Timoshenko beam theory with the dynamic stiffness approach (Subsection 4.6). These four methods incorporate an increasing degree of generality of underlying dynamic deformation of the beam within the unit cell. Timoshenko beam theory with the dynamic stiffness approach offers the most flexible deformation pattern and consequently, its resonance peak is at the lowest frequency in Fig. 15. A clear aspect can be seen from this figure is the striking difference between the dynamic finite element and the dynamic stiffness approaches for higher normalised frequency values ($\omega/\omega_0 \geq 10$). This difference is attributed to the fact that the dynamic finite element method uses only one 'finite element' obtained using the static shape functions of the beam, while the dynamic stiffness approach uses exact frequency-dependent dynamic shape functions. Effective elastic moduli and Poisson's ratio of the lattice obtained using the dynamic stiffness approach, with both the Euler-Bernoulli and Timoshenko beam theories, are exact and can be considered as benchmark results in Fig. 15.

## 5. Generalisation to further geometries and shapes

The inclusion of stretching and shear deformation in the formulation allow the proposed analytical framework to be applied to various other lattice patterns and geometry of the constituent members, as discussed in Fig. 1. Below we give the details for some special cases of wide

interest.

### 5.1. Rectangular lattice: $\theta = 0$

The rectangular lattice is obtained when $\theta = 0$. The unit cell and the corresponding lattice material can be imagined from Fig. 1. Therefore, taking the limit $\theta \to 0$ in Eqs. ((54), (57), (64) and (67) we have

$$E_1(\omega) = \lim_{\theta\to 0} \frac{K_{55}(\omega)\cos\theta}{b(\beta+\sin\theta)\sin^2\theta\left(1+\cot^2\theta\frac{K_{55}(\omega)}{K_{44}(\omega)}\right)} = \frac{K_{44}(\omega)}{b\beta} \tag{161}$$

$$E_2(\omega) = \lim_{\theta\to 0} \frac{K_{55}(\omega)(\beta+\sin\theta)}{b\cos^3\theta\left(1+\tan^2\theta\frac{K_{55}(\omega)}{K_{44}(\omega)}+2\sec^2\theta\frac{K_{55}(\omega)}{K_{44}^{(h)}(\omega)}\right)} = \frac{K_{55}(\omega)\beta}{b\left(1+2\frac{K_{55}(\omega)}{K_{44}^{(h)}(\omega)}\right)} \tag{162}$$

$$\nu_{12}(\omega) = \lim_{\theta\to 0} \frac{\cos^2\theta\left(1-\frac{K_{55}(\omega)}{K_{44}(\omega)}\right)}{(\beta+\sin\theta)\sin\theta\left(1+\cot^2\theta\frac{K_{55}(\omega)}{K_{44}(\omega)}\right)} = 0 \tag{163}$$

$$\nu_{21} = \lim_{\theta\to 0} \frac{(\beta+\sin\theta)\sin\theta\left(1-\frac{K_{55}(\omega)}{K_{44}(\omega)}\right)}{\cos^2\theta\left(1+\tan^2\theta\frac{K_{55}(\omega)}{K_{44}(\omega)}+2\sec^2\theta\frac{K_{55}(\omega)}{K_{44}^{(h)}(\omega)}\right)} = 0 \tag{164}$$

For a rectangular lattice, the Poisson's ratio in both the directions are effectively zero. The shear modulus can be obtained as

$$G_{12}(\omega) = \lim_{\theta\to 0}\frac{(\beta+\sin\theta)}{b\cos\theta}\frac{1}{\left(-\frac{h^2}{2lK_{65}(\omega)}+\frac{4K_{66}^{(h/2)}(\omega)}{\left(K_{55}^{(h/2)}(\omega)K_{66}^{(h/2)}(\omega)-\left(K_{56}^{(h/2)}(\omega)\right)^2\right)}+\frac{(\cos\theta+(\beta+\sin\theta)\tan\theta)^2}{K_{44}(\omega)}\right)}$$
$$= \frac{\beta}{b}\frac{1}{\left(-\frac{h^2}{2lK_{65}(\omega)}+\frac{4K_{66}^{(h/2)}(\omega)}{\left(K_{55}^{(h/2)}(\omega)K_{66}^{(h/2)}(\omega)-\left(K_{56}^{(h/2)}(\omega)\right)^2\right)}+\frac{1}{K_{44}(\omega)}\right)} \tag{165}$$

For the case of static Timoshenko beam, the equivalent elastic moduli for the rectangular lattice can be obtained as $E_1 = E\alpha/\beta, E_2 = E\alpha^3\beta/(1+2\alpha^2\beta+\Phi), G_{12} = E\alpha^3\beta/(\beta^2(2\beta+1+\Phi)+8\Phi\beta+\alpha^2)$. Similar expressions can be readily obtained using Euler-Bernoulli beam theory. It is worthy to note that the effective elastic properties of a rectangular lattice needs to incorporate the axial deformation since it is the most significant deformation mechanism in such lattices.

### 5.2. Auxetic lattice: $\theta$ is negative

The auxetic or re-entrant lattice is obtained when the angle θ is negative. The unit cell and the corresponding lattice material is shown in Fig. 1(e). Therefore, taking the case $\theta = -\theta$ in Eqs. ((54), (57), (64) and (67) we have

$$E_1(\omega) = \frac{K_{55}(\omega)\cos\theta}{b(\beta-\sin\theta)\left(\sin^2\theta+\cos^2\theta\frac{K_{55}(\omega)}{K_{44}(\omega)}\right)} \tag{166}$$

$$E_2(\omega) = \frac{K_{55}(\omega)(\beta-\sin\theta)}{b\cos\theta\left(\cos^2\theta+\sin^2\theta\frac{K_{55}(\omega)}{K_{44}(\omega)}+2\frac{K_{55}(\omega)}{K_{44}^{(h)}(\omega)}\right)} \tag{167}$$

$$\nu_{12}(\omega) = -\frac{\cos^2\theta\left(1-\frac{K_{55}(\omega)}{K_{44}(\omega)}\right)}{(\beta-\sin\theta)\sin\theta\left(1+\cot^2\theta\frac{K_{55}(\omega)}{K_{44}(\omega)}\right)} \tag{168}$$

$$\nu_{21} = -\frac{(\beta-\sin\theta)\sin\theta\left(1-\frac{K_{55}(\omega)}{K_{44}(\omega)}\right)}{\left(\cos^2\theta+\sin^2\theta\frac{K_{55}(\omega)}{K_{44}(\omega)}+2\frac{K_{55}(\omega)}{K_{44}^{(h)}(\omega)}\right)} \tag{169}$$

The shear modulus can also be obtained as

$$G_{12}(\omega) = \frac{(\beta-\sin\theta)}{b\cos\theta}\frac{1}{\left(-\frac{h^2}{2lK_{65}(\omega)}+\frac{4K_{66}^{(h/2)}(\omega)}{\left(K_{55}^{(h/2)}(\omega)K_{66}^{(h/2)}(\omega)-\left(K_{56}^{(h/2)}(\omega)\right)^2\right)}+\frac{(\cos\theta-(\beta-\sin\theta)\tan\theta)^2}{K_{44}(\omega)}\right)} \tag{170}$$

### 5.3. Rhombus lattice: $h = \beta = 0$

The rhombus lattice is obtained when $h = \beta = 0$. This implies the absence of the vertical member in the unit cell in Fig. 2. The revised unit cell and the corresponding lattice material is shown in Fig. 1(h). For simplicity, only static Timoshenko beam is used as an example case. Extension to other element type follow a similar approach describe before. Therefore, taking the limit $\beta = 0$ in Eqs. (114)–(117) we have

$$E_1 = \lim_{\beta\to 0}\frac{E\alpha^3\cos\theta}{(\beta+\sin\theta)\left((1+\Phi)\sin^2\theta+\alpha^2\cos^2\theta\right)} = \frac{E\alpha^3\cos\theta}{\sin\theta\left((1+\Phi)\sin^2\theta+\alpha^2\cos^2\theta\right)} \tag{171}$$

$$E_2 = \lim_{\beta\to 0}\frac{E\alpha^3(\beta+\sin\theta)}{(1+\Phi-\alpha^2)\cos^3\theta+\alpha^2(2\beta+1)\cos\theta} = \frac{E\alpha^3\sin\theta}{\cos\theta\left((1+\Phi)\cos^2\theta+\alpha^2\sin^2\theta\right)} \tag{172}$$

$$\nu_{12} = \lim_{\beta\to 0}\frac{\cos^2\theta(1+\Phi-\alpha^2)}{(\beta+\sin\theta)\sin\theta(1+\Phi+\alpha^2\cot^2\theta)} = \frac{\cos^2\theta(1+\Phi-\alpha^2)}{(1+\Phi)\sin^2\theta+\alpha^2\cos^2\theta} \tag{173}$$

$$\nu_{21} = \lim_{\beta\to 0}\frac{(\beta+\sin\theta)\sin\theta(1+\Phi-\alpha^2)}{(1+\Phi-\alpha^2)\cos^2\theta+\alpha^2(2\beta+1)} = \frac{\sin^2\theta(1+\Phi-\alpha^2)}{\left((1+\Phi)\cos^2\theta+\alpha^2\sin^2\theta\right)} \tag{174}$$

The shear modulus can be obtained in a similar manner from Eq. (120) as

$$G_{12}(\omega) = \lim_{\beta\to 0}\frac{E\alpha^3(\beta+\sin\theta)}{\left(\beta^2(1+\Phi+2\beta)+8\beta\Phi+\alpha^2(\cos\theta+(\beta+\sin\theta)\tan\theta)^2\right)\cos\theta} = E\alpha\sin\theta\cos\theta \tag{175}$$

### 5.4. Other two and three dimensional lattices

In the last three subsections, we have shown how the closed-form formulae of effective elastic properties of hexagonal lattices can be directly converted to different other lattice forms. In principle, the dynamic stiffness based framework incorporating bending, shear and axial deformation can be utilized to all other two and three dimensional lattices, which may not be directly deducible from a hexagonal lattice (for example, refer to the triangular lattice shown in Fig. 1(i)). In such cases, an appropriate unit cell needs to be identified and the same dynamic stiffness matrix for a beam element can be used to find the effective elastic properties following a similar analytical framework.

### 5.5. Lattice with non-prismatic general elements

The analytical formulations outlined so far consider prismatic beam elements as constituent members of the lattice. This implies that the properties of the beam do not change along the length of the beam. However, to consider beams with variable cross-section as outlined earlier in Fig. 1(d) or beams made of advanced materials such as composite materials (Sather and Krishnamurthy, 2019), a more general approach is necessary. In Fig. 16 a beam element with arbitrary variable

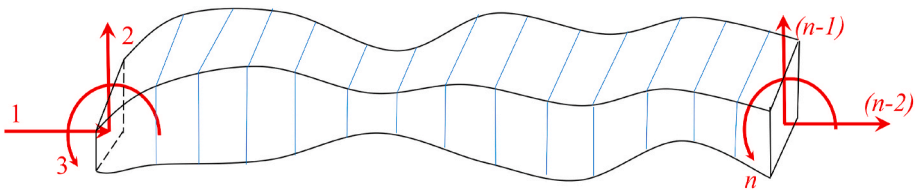


**Fig. 16.** A 2D beam element with arbitrary variable cross section. The beam element is discretised using the finite element method. There are a total of six degrees of freedom at the two end nodes. The degrees of freedom in each node correspond to the axial, transverse and rotational deformation.

cross section is shown. This general element is a constituent beam-like member of the entire lattice under consideration. As we are interested only in the in-plane properties of the lattice, the consideration of two-dimensional deformation is sufficient. The 2D beam element can be discretised in a finite number of elements. We propose a dynamic condensation approach for this general case such that the stiffness element components corresponding to only the end degree of freedom are needed to be considered. This will essentially pave the way to utilize the analytical framework presented in this article in terms of the stiffness matrix of the constituent beam elements for finding out the effective elastic properties of the entire lattice.

For dynamic analysis using the finite element method, the dynamic equilibrium equation corresponding to the beam element in Fig. 16 can be expressed as

$$\mathbf{D}(\omega)\mathbf{U}(\omega) = \mathbf{f}(\omega) \tag{176}$$

Here $\mathbf{U}(\omega) \in \mathrm{C}^n$ and $\mathbf{f}(\omega) \in \mathrm{C}^n$ are respectively the nodal displacement and applied forcing vector on the element. In general both vectors are complex valued and the total degree of freedom $n > 6$ due to the fine discretization of the beam element. Using the $n \times n$ mass, damping and stiffness matrices, the element dynamic matrix can be obtained as

$$\mathbf{D}(\omega) = -\omega^2\mathbf{M} + \mathrm{i}\omega\mathbf{C} + \mathbf{K} \tag{177}$$

We denote

$$\begin{aligned} &\mathbf{U}_e(\omega) = \{U_1(\omega), U_2(\omega), U_3(\omega), U_{n-2}(\omega), U_{n-1}(\omega), U_n(\omega)\}^T \in \mathrm{C}^6 \\ &\text{and} \quad \mathbf{f}_e(\omega) = \{f_1(\omega), f_2(\omega), f_3(\omega), f_{n-2}(\omega), f_{n-1}(\omega), f_n(\omega)\}^T \in \mathrm{C}^6 \end{aligned} \tag{178}$$

as the displacement and applied forcing vector on the element corresponding to the two end nodes, respectively. Recall that the analytical formulation derived in Section 3 only requires a direct relationship between these two vectors. To obtain this relationship, we partition the overall dynamic matrix in Eq. (177) and rewrite the dynamic equilibrium equation as

$$\begin{bmatrix} \mathbf{D}_{ee}(\omega) & \mathbf{D}_{ei}(\omega) \\ \mathbf{D}_{ie}(\omega) & \mathbf{D}_{ii}(\omega) \end{bmatrix} \begin{Bmatrix} \mathbf{U}_e(\omega) \\ \mathbf{U}_i(\omega) \end{Bmatrix} = \begin{Bmatrix} \mathbf{f}_e(\omega) \\ \mathbf{0} \end{Bmatrix} \tag{179}$$

In the above equation subscript $i$ denotes internal degrees of freedom and subscript $e$ denotes end degrees of freedom. The dimensions of the matrices and vectors in the above equation are given by $\mathbf{U}_i(\omega) \in \mathrm{C}^{(n-6)}$, $\mathbf{D}_{ei}(\omega) \in \mathrm{C}^{6\times(n-6)}$, $\mathbf{D}_{ie}(\omega) \in \mathrm{C}^{(n-6)\times 6}$ and $\mathbf{D}_{ii}(\omega) \in \mathrm{C}^{(n-6)\times(n-6)}$. As there is no internal forcing, the vector corresponding to $\mathbf{f}_i(\omega)$ is $0 \in \mathrm{R}^{(n-6)}$.

Eliminating the internal degree of freedom $\mathbf{U}_i(\omega)$, from Eq. (179) we obtain the direct relationship between end nodal forces and displacements as

$$\underbrace{\left[\mathbf{D}_{ee}(\omega) - \mathbf{D}_{ei}(\omega)\mathbf{D}_{ii}^{-1}(\omega)\mathbf{D}_{ie}(\omega)\right]}_{\mathbf{D}_s(\omega)\in\mathrm{C}^{6\times6}} \mathbf{U}_e(\omega) = \mathbf{f}_e(\omega) \tag{180}$$

The elements of the above condensed dynamic matrix $\mathbf{D}_s(\omega)$ can be used in the analytical expressions derived in Section 3 to obtain the equivalent elastic moduli and Poisson's ratio of the lattices with any general beam element. Further, the above approach couple be used to account for the effect of spatially varying intrinsic material properties within the constituting beam elements. Therefore, the proposed analytical framework in this article is not only generic in terms of the band of vibration frequency and lattice geometry, but it is also capable of accounting any non-prismatic spatially varying beam shapes and intrinsic material properties.

## 6. Conclusions and perspective

An augmented dynamic stiffness approach based generic analytical framework is presented for analysing the elastic moduli of lattice materials under steady-state vibration conditions. In a vibrating condition, the frequency-dependent local deformation mechanism of the constituent beam-like elements of a lattice leads to a completely different deformation behaviour at the global level compared to the static condition. Here we propose to exploit the possibility of modulating the elastic properties of the lattices as a function of the ambient vibration. An analytical framework leading to the development of closed-form expressions for the frequency-dependent elastic moduli, as derived in this article, provides a computationally efficient and physically insightful approach for investigating the global lattice behaviour under dynamic conditions. Such computational efficiency can be particularly appealing for developing multi-functional engineered material microstructures where multiple realizations are often needed in an inverse identification framework.

The stretching-enriched physics of deformation in the lattice materials in addition to the bending and shear deformations under dynamic conditions lead to complex elastic moduli due to the presence of damping. This has been exactly captured using the proposed dynamic stiffness based framework, which is valid over any frequency ranges. The dynamic stiffness method employs exact frequency-adaptive shape functions to represent the deformation of the unit cell in the lattice. In the context of wave propagation, this captures the sub-wavelength scale dynamics. Dependence of Poisson's ratio on the intrinsic material physics in case of a geometrically regular lattice, as unravelled in this article, is in contrary to the common notion that Poisson's ratios of perfectly periodic lattices are the only function of the microstructural geometry. The article systematically shows that the proposed expressions of elastic moduli exactly reduce to the previously reported formulae for special cases of neglecting the axial and shear deformation effect under the dynamic condition as well as the standard formulae for hexagonal honeycombs when the vibrating frequency tends to zero (i.e. static deformation). This essentially provides exact analytical validations for the proposed formulae corresponding to static and dynamic conditions. Detailed analytical derivations of the most general to the several special cases are shown including the static finite element, dynamic finite element and dynamic stiffness considering Euler-Bernoulli and Timoshenko beam theory.

Novelty of this paper includes the development of generalized closed-form analytical expressions for frequency-dependent elastic moduli of lattice materials under dynamic condition including the effect of axial and shear deformation. The chronological development of the effective elastic moduli as systematically presented in this paper may be noted. For the sake of completeness and maintaining the flow of a comprehensive presentation, we start with the static stiffness matrices of

a single beam for both Euler-Bernoulli and Timoshenko beam theories, which are used in the following step to derive the closed form expressions of the effective elastic moduli of the entire lattice under static condition. The dynamic elastic moduli of the lattices are also presented following Euler-Bernoulli and Timoshenko beam theories in the framework of dynamic stiffness matrix and dynamic finite element matrix. It is clearly explained that the formulations based on Timoshenko beam theory is more generic than the Euler-Bernoulli beam theory both in static and dynamic conditions, while the dynamic stiffness based approach can cover wider range of frequencies compared to the dynamic finite element formulation. The closed-form analytical formulae for the dynamic elastic moduli of lattices including shear and axial deformations are reported for the first time in this article.

The attractiveness of this article lies in the generality and comprehensiveness of the proposed analytical framework, which would have a broad impact on artificially engineered materials development. The analytical framework reported here is the most general to date; it is applicable to (a) any form of two or three dimensional lattices (though we have focused on a set of two dimensional lattices, the generic dynamic stiffness based framework can be readily extended to other lattice forms following a similar approach), (b) any profile of the constituent beam-like elements due to inclusion of axial and shear deformation effects (different cross sections as well as spatially varying geometry and intrinsic material properties), (c) a wide range of frequency band covering low (including zero) to high frequencies, and (d) dynamic systems including the effect of intrinsic material damping. Most of the research activities in the field of lattice metamaterials dealing with elastic properties revolve around intuitively designing the microstructural geometry of the lattice structure. Here we develop the necessary analytical framework to couple the physics of deformation as a function of vibrating frequency along with the conventional approach of designing microstructural geometry to expand the effective design space significantly. The efficient and elegant, yet physically insightful closed-form formulae along with the generic analytical approach, proposing new exploitable dimensions in the engineered materials research, would lead to unravelling unprecedented material properties for modern multi-functional structural systems across the length-scales.

## Author agreement statement

1. We the undersigned declare that this manuscript is original, has not been published before and is not currently being considered for publication elsewhere.
2. We confirm that the manuscript has been read and approved by all named authors and that there are no other persons who satisfied the criteria for authorship but are not listed. We further confirm that the order of authors listed in the manuscript has been approved by all of us.
3. We understand that the Corresponding Author is the sole contact for the Editorial process. He/she is responsible for communicating with the other authors about progress, submissions of revisions and final approval of proofs

## Declaration of competing interest

The authors declare that they have no known competing financial interests or personal relationships that could have appeared to influence the work reported in this paper.

## Acknowledgements

SA gratefully acknowledges the financial support from the European Commission under the Marie Skodowska Curie Actions (grant number 799201- METACTIVE). TM acknowledges the initiation grant received from IIT Kanpur during the research work. XL appreciates the financial supports from the National Natural Science Foundation of China (Grant No. 11802345) and State Key Laboratory of High Performance Complex Manufacturing (Grant No. ZZYJKT2019-07). SA and XL also acknowledges the financial support from the High-end foreign expert introduction project through Grant no G20190018004.

## References

Adhikari, S., 2013. Structural Dynamic Analysis with Generalized Damping Models: Analysis. Wiley ISTE, UK, p. 368.
Adhikari, S., Mukhopadhyay, T., Shaw, A., Lavery, N., 2020. Apparent negative values of youngâ€™s moduli of lattice materials under dynamic conditions. Int. J. Eng. Sci. 150, 103231.
Berger, J.B., Wadley, H.N.G., McMeeking, R.M., 2017. Mechanical metamaterials at the theoretical limit of isotropic elastic stiffness. Nature 543 (7646), 533–537.
Bhat, S.K., Ganguli, R., 2019. Nonuniform isospectrals of uniform timoshenko beams. AIAA J. 57 (11), 4927–4941.
Bigoni, D., Guenneau, S., Movchan, A.B., Brun, M., 2013. Elastic metamaterials with inertial locally resonant structures: application to lensing and localization. Phys. Rev. B 87, 174303.
Brillouin, L., 1953. Wave Propagation in Periodic Structures. Dover Publications, New York, USA.
Buckmann, T., Thiel, M., Kadic, M., Schittny, R., Wegener, M., 2014. An elasto-mechanical unfeelability cloak made of pentamode metamaterials. Nat. Commun. 5, 4130.
Chandra, Y., Mukhopadhyay, T., Adhikari, S., Figiel, F., 2020. Size-dependent dynamic characteristics of graphene based multi-layer nano hetero-structures. Nanotechnology 31, 145705.
Chen, Y., Hu, G., Huang, G., 2017. A hybrid elastic metamaterial with negative mass density and tunable bending stiffness. J. Mech. Phys. Solid. 105, 179–198.
R. V. Craster, J. Kaplunov, A. V. Pichugin, High-frequency homogenization for periodic media, Proceedings of the Royal Society of London A: Mathematical, Physical and Engineering Sciences.doi:10.1098/rspa.2009.0612.
Dawe, D., 1984. Matrix and Finite Element Displacement Analysis of Structures. Oxford University Press, Oxford, UK.
Deymier, P.A., 2013. Acoustic Metamaterials and Phononic Crystals, Springer Series in Solid-State Sciences, vol. 173. Springer, New York, USA.
El-Sayed, F.K.A., Jones, R., Burgess, I.W., 1979. A theoretical approach to the deformation of honeycomb based composite materials. Composites 10 (4), 209–214.
Fang, N., Xi, D., Xu, J., Ambati, M., Srituravanich, W., Sun, C., Zhang, X., 2006. Ultrasonic metamaterials with negative modulus. Nat. Mater. 5 (6), 452–456.
García-Chocano, V.M., Christensen, J., Sánchez-Dehesa, J., 2014. Negative refraction and energy funneling by hyperbolic materials: an experimental demonstration in acoustics. Phys. Rev. Lett. 112, 144301.
Gibson, L., Ashby, M.F., 1999. Cellular Solids Structure and Properties. Cambridge University Press, Cambridge, UK.
Gopalakrishnan, S., Chakraborty, A., Mahapatra, D.R., 2008. Spectral Finite Element Method. Springer-Verlag, London.
Hashin, Z., Shtrikman, S., 1963. A variational approach to the theory of the elastic behaviour of multiphase materials. J. Mech. Phys. Solid. 11 (2), 127–140.
Hussein, M.I., 2009a. Reduced Bloch mode expansion for periodic media band structure calculations. Proc. Roy. Soc. Lond.: Mathematical, Physical and Engineering Sciences 465 (2109), 2825–2848.
Hussein, M.I., 2009b. Theory of damped Bloch waves in elastic media. Phys. Rev. B 80, 212301.
Hussein, M.I., Frazier, M.J., 2013. Metadamping: an emergent phenomenon in dissipative metamaterials. J. Sound Vib. 332 (20), 4767–4774.
Hussein, M.I., Leamy, M.J., Ruzzene, M., 2014. Dynamics of phononic materials and structures: historical origins, recent progress, and future outlook. Appl. Mech. Rev. 66 (4), 040802–38.
Kadic, M., Buckmann, T., Stenger, N., Thiel, M., Wegener, M., 2012. On the practicability of pentamode mechanical metamaterials. Appl. Phys. Lett. 100 (19), 191901.
Karlicic, D., Cajic, M., Chatterjee, T., Adhikari, S., 2021. Wave propagation in mass embedded and pre-stressed hexagonal lattices. Compos. Struct. 256 (1), 113087.
Koloušek, V., 1941. Anwendung des Gesetzes der virtuellen Verschiebungen und des Reziprozitätssatzes in der Stabwerksdynamik. Ing. Arch. 12 (6), 363–370.
Lakes, R., 1987. Foam structures with a negative Poisson's ratio. Science 235 (4792), 1038–1040.
Lee, U., 2009. Spectral Element Method in Structural Dynamics. John Wiley & Sons, Singapore.
Leung, A.Y.T., 1993. Dynamic Stiffness and Substructures. Springer London, London.
Liu, X., Hu, G., Sun, C., Huang, G., 2011. Wave propagation characterization and design of two-dimensional elastic chiral metacomposite. J. Sound Vib. 330 (11), 2536–2553.
Malek, S., Gibson, L., 2015. Effective elastic properties of periodic hexagonal honeycombs. Mech. Mater. 91, 226–240.
Masters, I., Evans, K., 1996. Models for the elastic deformation of honeycombs. Compos. Struct. 35 (4), 403–422.
Mead, D., 1996. Wave propagation in continuous periodic structures: research contributions from southampton, 1964-1995. J. Sound Vib. 190 (3), 495–524.
Meza, L.R., Phlipot, G.P., Portela, C.M., Maggi, A., Montemayor, L.C., Comella, A., Kochmann, D.M., Greer, J.R., 2017. Reexamining the mechanical property space of three-dimensional lattice architectures. Acta Mater. 140, 424–432.
Milton, G.W., Briane, M., Willis, J.R., 2006. On cloaking for elasticity and physical equations with a transformation invariant form. New J. Phys. 8 (10), 248.

Mukhopadhyay, T., Adhikari, S., 2016a. Effective in-plane elastic properties of auxetic honeycombs with spatial irregularity. Mech. Mater. 95, 204–222.
Mukhopadhyay, T., Adhikari, S., 2016b. Free vibration analysis of sandwich panels with randomly irregular honeycomb core. J. Eng. Mech. 142 (11), 06016008.
Mukhopadhyay, T., Adhikari, S., 2017a. Stochastic mechanics of metamaterials. Compos. Struct. 162, 85–97.
Mukhopadhyay, T., Adhikari, S., 2017b. Effective in-plane elastic properties of quasi-random spatially irregular hexagonal lattices. Int. J. Eng. Sci. 119 (10), 142–179.
Mukhopadhyay, T., Mahata, A., Adhikari, S., Asle Zaeem, M., 2017a. Effective mechanical properties of multilayer nano-heterostructures. Sci. Rep. 7, 15818.
Mukhopadhyay, T., Mahata, A., Adhikari, S., Zaeem, M.A., 2017b. Effective elastic properties of two dimensional multiplanar hexagonal nanostructures. 2D Mater. 4 (2), 025006.
Mukhopadhyay, T., Mahata, A., Adhikari, S., Asle Zaeem, M., 2018. Probing the shear modulus of two-dimensional multiplanar nanostructures and heterostructures. Nanoscale 10, 5280–5294.
Mukhopadhyay, T., Adhikari, S., Batou, A., 2019a. Frequency domain homogenization for the viscoelastic properties of spatially correlated quasi-periodic lattices. Int. J. Mech. Sci. 150, 784–806.
Mukhopadhyay, T., Adhikari, S., Alu, A., 2019b. Probing the frequency-dependent elastic moduli of lattice materials. Acta Mater. 165, 654–665.
Mukhopadhyay, T., Adhikari, S., Alu, A., 2019c. Theoretical limits for negative elastic moduli in subacoustic lattice materials. Phys. Rev. B 99, 094108.
Mukhopadhyay, T., Ma, J., Feng, H., Hou, D., Gattas, J.M., Chen, Y., You, Z., 2020a. Programmable stiffness and shape modulation in origami materials: emergence of a distant actuation feature. Applied Materials Today 19, 100537.
Mukhopadhyay, T., Naskar, S., Adhikari, S., 2020b. Anisotropy tailoring in geometrically isotropic multi-material lattices. Extreme Mechanics Letters 40, 100934.
Mukhopadhyay, T., Mahata, A., Naskar, S., Adhikari, S., 2020c. Probing the effective Young's modulus of 'magic angle' inspired multi-functional twisted nano-heterostructures. Advanced Theory and Simulations 3 (10), 2000129.
Nemat-Nasser, S., Willis, J.R., Srivastava, A., Amirkhizi, A.V., 2011. Homogenization of periodic elastic composites and locally resonant sonic materials. Phys. Rev. B 83, 104103.
Norris, A.N., Shuvalov, A.L., Kutsenko, A.A., 2012. Analytical formulation of three-dimensional dynamic homogenization for periodic elastic systems. Proc. Roy. Soc. Lond.: Mathematical, Physical and Engineering Sciences 468 (2142), 1629–1651. https://doi.org/10.1098/rspa.2011.0698.
Palermo, A., Marzani, A., 2016. Extended bloch mode synthesis: ultrafast method for the computation of complex band structures in phononic media. Int. J. Solid Struct. 100, 29–40.
Paz, M., 1980. Structural Dynamics: Theory and Computation, second ed. Van Nostrand, Reinhold.
Petyt, M., 1990. Introduction to Finite Element Vibration Analysis. Cambridge University Press, Cambridge, UK.
Pivovarov, D., Steinmann, P., 2016a. Modified sfem for computational homogenization of heterogeneous materials with microstructural geometric uncertainties. Comput. Mech. 57 (1), 123–147.
Pivovarov, D., Steinmann, P., 2016b. On stochastic fem based computational homogenization of magneto-active heterogeneous materials with random microstructure. Comput. Mech. 58 (6), 981–1002.
Rivello, R.M., 1969. Theory and Analysis of Flight Structures, first ed. McGraw-Hill, New York.
Roy, A., Gupta, K.K., Naskar, S., Mukhopadhyay, T., Dey, S., 2021. Compound influence of topological defects and heteroatomic inclusions on the mechanical properties of SWCNTs. Materials Today Communications 26, 102021.
Sather, E., Krishnamurthy, T., April 2019. An Analytical Method to Calculate Effective Elastic Properties of General Multifunctional Honeycomb Cores in Sandwich Composites, Tech. Rep. NASA/TM-02019€-220275. NASA, Langley Research Center, Hampton, Virginia.
Singh, A., Mukhopadhyay, T., Adhikari, S., Bhattacharya, B., 2021. Voltage-dependent modulation of elastic moduli in lattice metamaterials: emergence of a programmable state-transition capability. Int. J. Solid Struct. 208–209, 31–48.
Srivastava, A., 2015. Elastic metamaterials and dynamic homogenization: a review. Int. J. Smart Nano Mater. 6 (1), 41–60.
Stenger, N., Wilhelm, M., Wegener, M., 2012. Experiments on elastic cloaking in thin plates. Phys. Rev. Lett. 108, 014301.
Sugino, C., Leadenham, S., Ruzzene, M., Erturk, A., 2016. On the mechanism of bandgap formation in locally resonant finite elastic metamaterials. J. Appl. Phys. 120 (13), 134501.
Wang, H., Zhao, D., Jin, Y., Wang, M., Mukhopadhyay, T., You, Z., 2020. Modulation of multi-directional auxeticity in hybrid origami metamaterials. Applied Materials Today 20, 100715.
Wehmeyer, S., Zok, F.W., Eberl, C., Gumbsch, P., Cohen, N., McMeeking, R.M., Begley, M.R., 2019. Post-buckling and dynamic response of angled struts in elastic lattices. J. Mech. Phys. Solid. 133, 103693.
Willis, J., 2009. Exact effective relations for dynamics of a laminated body. Mech. Mater. 41 (4), 385–393 (the Special Issue in Honor of Graeme W. Milton).
Yang, Z., Mei, J., Yang, M., Chan, N.H., Sheng, P., 2008. Membrane-type acoustic metamaterial with negative dynamic mass. Phys. Rev. Lett. 101, 204301.
Yu, F., Collet, M., Ichchou, M., Lin, L., Bareille, O., Dimitrijevic, Z., 2017. Enhanced wave and finite element method for wave propagation and forced response prediction in periodic piezoelectric structures. Chin. J. Aeronaut. 30 (1), 75–87.
Zheng, X., Lee, H., Weisgraber, T.H., Shusteff, M., DeOtte, J., Duoss, E.B., Kuntz, J.D., Biener, M.M., Ge, Q., Jackson, J.A., Kucheyev, S.O., Fang, N.X., Spadaccini, C.M., 2014. Ultralight, ultrastiff mechanical metamaterials. Science 344 (6190), 1373–1377.
Zhu, R., Liu, X.N., Hu, G.K., Sun, C.T., Huang, G.L., 2014. Negative refraction of elastic waves at the deep-subwavelength scale in a single-phase metamaterial. Nat. Commun. 5, 5510. EP.
Zhu, R., Chen, Y., Wang, Y., Hu, G., Huang, G., 2016. A single-phase elastic hyperbolic metamaterial with anisotropic mass density. J. Acoust. Soc. Am. 139 (6), 3303–3310.
Zok, F.W., Latture, R.M., Begley, M.R., 2016. Periodic truss structures. J. Mech. Phys. Solid. 96, 184–203.
Zschernack, C., Wadee, M.A., Vollmecke, C., 2016. Nonlinear buckling of fibre-reinforced unit cells of lattice materials. Compos. Struct. 136, 217–228.